The Thesis Committee for Adriana Jocelyn Da Costa
Certifies that this is the approved version of the following thesis:

Skeletal muscle repair following Plantar nerve relocation on an extracellular matrix seeded with mesenchymal stem cells in a PEGylated fibrin gel as a treatment model for volumetric muscle loss.

APPROVED BY
SUPERVISING COMMITTEE:

Supervisor:

Roger P. Farrar

Wesley J. Thompson

Skeletal muscle repair following Plantar nerve relocation on an extracellular matrix seeded with mesenchymal stems cells in PEGylated fibrin gel as a treatment model for volumetric muscle loss.

by

Adriana Jocelyn Da Costa, B.S.

Thesis

Presented to the Faculty of the Graduate School of

The University of Texas at Austin

in Partial Fulfillment

of the Requirements

for the Degree of

Master of Science in Kinesiology

The University of Texas at Austin

August 2014

Dedication

This work is dedicated to my family, Phoenix, and all those who have supported and helped me throughout the years. A special thank you to my parents, Karen and Carlos without you I would not be where I am today.

Acknowledgements

This accomplishment would not have been possible without the help, support, and guidance from my advisor, Dr. Roger Farrar. Thank you for your knowledge, patience, and support Dr. Farrar and for believing in me as a student. I would also like to thank Dr. Wesley Thompson for his knowledge and expertise in the field of Neurobiology and for helping me learn and perfect the surgical techniques performed in my thesis, in particular the nerve relocation surgery. A tremendous thank you is in order for his animal contribution to our lab. A special thank you to Melissa Merscham-Banda for all her help these last few years, she was indispensible in teaching techniques and answering questions. A huge thank you to Eunhan Cho in helping with the tremendous task of data analysis, I could not have done it without you. Finally, I would like to thank all my present and former lab members in helping me throughout the years and making my time in lab enjoyable: Melissa Merscham, Eunhan Cho, Pei-Ling Hsieh, Viktoriya Rybalko, Chantal Pham, Kwang-Jun Lee, and TJ Song. Thank you to the rest of the Kinesiology department for your help and knowledge.

Abstract

Skeletal muscle repair following Plantar nerve relocation on an extracellular matrix seeded with mesenchymal stem cells in a PEGylated fibrin gel as a treatment model for volumetric muscle loss.

Adriana Jocelyn Da Costa, M.S. Kin

The University of Texas at Austin, 2014

Supervisor: Roger P. Farrar

The toll skeletal muscle injury, resulting in significant muscle mass loss, has on the patient reaches far more than physical and emotional, as the tolls are financial as well. Approximately more than 3 billion dollars is spent on the initial medical costs and on subsequent disability benefits, following a volumetric muscle loss. Skeletal muscle has a robust capacity for self-repair; this propensity for repair is hindered when skeletal muscle loss is larger than 20% of the total mass of the muscle. Previous work in our lab, has shown functional and morphological improvements following the cellular therapy, with mesenchymal stem cells (MSC), as well as with nerve relocation to the extracellular matrix (ECM). To further observe the regenerative properties of the above treatments, a defect weighing approximately 307 ± 3.7 mg wet weight and measuring approximately 1x 1cm² was removed from the lateral gastrocnemius (LGAS) of male Sprague Dawley rats. Additionally, the medial branch of the plantar nerve was then relocated and implanted to the middle of the ECM. Seven days post injury bone-marrow derived

mesenchymal stem cells were injected directly into the implant using a PEGylated Fibrin hydrogel (PEG). Following 56 days of recovery, partial functional restoration was observed in the LGAS ECM seeded with MSC and implanted with the plantar nerve. The LGAS produced 86.3 ± 5.8% of the contralateral LGAS, a value that was significantly higher than ECM implantation alone ($p < .05$). The implanted ECM seeded with MSC and implanted with the plantar nerve showed significant increases in blood vessel density and myofiber content ($p < .05$). The data suggest that a volumetric injury can be repaired by neurotization of an implanted muscle-derived ECM seeded with MSCs.

Table of Contents

List of Figures

INTRODUCTION

Degenerative diseases, surgical ablations, traumatic motor vehicle accidents, traumatic injuries caused by improvised explosive devices (IEDs), and gunshot wounds in both civilian and military populations often result in severe muscle loss. In 2014 alone, the department of defense has appropriated 30 million dollars to support research focused on restoring function of orthopedic injuries sustained by military personal in combat. The research done for injuries in military populations can also translate to civilian populations. The aforementioned injuries, often characterized by severe soft tissue damage, significant loss in tissue mass and functional deficits fall under injuries known as volumetric muscle loss (VML) (Grogan and Hsu, 2011). Despite significant losses in mass and function, as well as physical and aesthetic discomfort to the patient, there is no clinical standard for VML, and therapeutic advances have been limited to the use of carbon-fiber braces and autologous functional free muscle transfer (Grogan and Hsu, 2011, Fan et *al.,* 2008, Li et al., 2013). Clinical treatments are limited to injuries occurring below the knee or in other similar extremeties, apply only to small areas of tissue, and risk donor site morbidity and loss of function (Grogan and Hsu, 2011, Tu et *al*. 2008, Fan et *al.,* 2008). Another caveat of free muscle transfer is that the donor muscle must meet special requirements in length, fiber characteristics, point of origin and insertion, as well as meet certain specification in vascular and neural supply to be considered for donation. Characteristics that limit possible donor muscles to a few type 1 muscles (Zuker and Manktelow, 2007). Free muscle transfers have been met with varying

results. Roughly four-fifths of patients receiving a free muscle transfer are able to regain full elbow flexion, yet some experience difficulty in regaining functional strength when flexion is tested with a 3lb weight (Seal and Stevanovich, 2011, Zuker and Manktelow, 2007). These varying results in functional measures make the search for clinical alternatives imperative to the treatment of VML.

Skeletal muscle, composed of myofibers and connective tissue, heals through an intrinsic repair process in which a normally quiescent population of cells, known as satellite cells, becomes activated upon injury. These cells which normally reside under the basal lamina proliferate, then differentiate into myoblasts, and subsequently fuse together to form myotubes (Jarvinen et *al.*, 2005). The process of self repair becomes hindered when the area between the ruptured stumps is insurmountable, leaving the remaining muscle fibers unable to fuse together, as well as due to the formation of extraneous scar tissue between the ruptured stumps (Huard et *al*. 2002). As is common in VML injuries, these problems in repair often leave the area devoid of muscle fibers or leave the tissue with a sizeable gap between muscle fibers (Merritt et *al*, 2010, Terada et *al*, 2001). Thus, a biocompatible material to bridge the gap between myofibers is paramount to the treatment of VML injury.

Orthopedic surgeons and civilian medical, as well as military personnel are faced with the task of repairing not only muscle tissue but collagen, nerve and vascular tissue after a VML injury. These challenges have led to research into biocompatible materials that might aid in reconnecting the remaining muscle fibers, diminish the need for autologous tissue, multiple surgical procedures, as well as produce an environment

conductive to angiogenesis and neurogenesis within the defect. Research in tissue engineering has looked at several autologous, non autologous/acellular grafts, as well as naturally based materials, and synthetic materials, as scaffolds for regeneration of both muscle and nerves from both the central nervous system and peripheral nervous system (Schmidt and Baier Leach, 2003). Hydrogels, collagen and laminin structures, polymer matrices and decellularized tissues are being researched with the aim of improving musculature, vasculature, and nerves within the matrix, as well as functional capacity of the tissue (Madaghiele et al, 2007, Li et *al.,* 2007). Porcine small intestinal submucosa (SIS) implantation as treatment for VML has shown promising results in regeneration in animal studies. However many studies using SIS have looked only at abdominal wall models of VML injury and few have focused on the use of SIS in the treatment of VML in load bearing muscles. Initial results have shown impaired regeneration, non functional muscle, bone and cartilage in the treatment of the vastus lateralis muscle following treatment with SIS (Turner et *al*., 2012). A clinical case study looked at SIS in the repair of a quadriceps femoris muscle and found soft tissue development within the muscle using CT scan, as well as improvement in isokinetic function following 36 weeks of recovery (Mase et al., 2010). The limitation in this study is that Biodex measures only the combined contribution of all muscles in the quadriceps, thus making it difficult to determine if the improved effects seen are isolated to an improvement in the vastus lateralis or a compensatory effect of the surrounding muscles. Although an improvement in isokinetic function and subjective self-assessment is shown, the data shows that

compared to the contralateral leg, function remains well below normal levels, showing a need for continued research in viable methods to increase and restore function.

Successful treatment utilizing scaffolds requires scaffolds to balance mechanical function, provide a modulus within (.4-350MPa), and deliver biofactors, which play a role in bone, soft tissue, and neural regeneration (Hollister, 2005). Research has suggested that using naturally based scaffolds in homologous sites aids in regeneration due to site- specific extracellular matrix (ECM) composition and structure, specifically the axially oriented pores (Wolf et *al.*, 2012, Madaghiele et *al.*, 2007). The innate structural characteristics of homologous ECM have made it an attractive option in the treatment of VML injuries. Extracellular matrices produced through the process of decellularization aid in remodeling of tissue through their recruitment of various cells to the site of injury; including inflammatory cells, stem and progenitor cells. The extracellular matrix three dimensional structure and array of structural and functional proteins help to dictate the topography and relocalization of synapses, blood vessels, and cells in the tissue (Singhal and Martin, 2011, Wolf et al., 2011, Badylak, S.F, 2007, Valentin et al, 2006). Additionally, studies have shown that ECMs containing fibronectin display enhanced motoneuron outgrowth, while on the other hand, laminin aids in the recruitment of Schwann cells (Gonzalez-Perez et al., 2013). While the innate characteristics of homologous ECM make it a viable option for treatment of VML, studies within our laboratory have shown limitations in regeneration in the middle fraction of the ECM, as well as significant deficits in function, when an ECM is

implanted alone (Merritt et al, 2010a, Merritt et al, 2010b). A combination of treatments is likely a solution for the impairments seen in treatment with ECM only.

Great importance has been placed on the use of bone marrow derived mesenchymal stem cells (BMSC) in the field of regenerative medicine due to the ease of isolation, expansion potential, differentiation ability into multiple cell lines, and migratory pattern to sites of injury (Ripoll and Bunnell, 2009, Pittenger and Martin, 2004). Furthermore, BMSCs can be autologously obtained which reduces the likelihood of eliciting an immune response; their lack of immunogenicity makes them an ideal candidate for regenerative treatment even when allogenically obtained (Pittenger and Martin, 2004). Various clinical and animal studies have looked at the role of BMSCs (both whole cell and cell extract) in myocardial infarction; these studies have shown improvements in function, following intravenous infusion despite embolism in the lung (Lee et al., 2009, Martin et al., 1999, Yeghiazarians et al., 2009). Additionally, BMSCs were found to express myogenic potential, as they have been found to express several myogenic transcription factors including pax 7, myoD, myogenin, myf-5 and myogenic proteins following transplantation (Dezawa et al., 2005, Pittenger and Martin, 2004, LaBarge and Blau, 2002). Although the exact methods by which BMSC contributes to muscle repair are unknown and debated, various studies have shown repair through repopulation of the satellite cell niche, varying levels of engraftment after culture on plastic or PEGylated fibrin hydrogel (PEG) wells, fusion, or through an autocrine/paracrine fashion via release of growth factors and chemokines that alter the environment (Prockop, 2003, Labarge and Blau, 2002, Gilbert et al., 2010, Dezawa et al,

2005, Palermo et al., 2005, Merritt et al., 2010a, Collins et al, 2005, Prockop, 2009, Gimbel et al., 2009). Bone marrow derived stem cells have been shown within our lab to aid in regeneration by increasing myofiber content, size, blood vessel density and function following 42 day and 56 day recovery post injury (Merscham et al., 2012 (unpublished), Sarathy et al, 2011 (unpublished), Tierney et al, 2009 (unpublished), Merritt et al, 2010a). Additionally, BMSC are shown to express an array of genes for all three germ layers, a characteristic important for treatment of VML injuries as nerve regeneration and vasculogenesis are important to the long term survival of muscle fibers (Woodbury et al., 2002). The ability of BMSC to differentiate into various tissues makes the topic of delivery to the injury site of importance.

In the past multiple bolus injections into the site of injury were the preferred method of growth factor and BMSC delivery, recently, however, tissue engineering has developed a synthetic material, polyethelene glycol conjugated to fibrin, PEGylated Fibrin (PEG-fib), which releases the covalently bound growth factors and BMSC in a temporally and spatially controlled manner from a single injection (Schmidt and Baeir Leach, 2003). PEGylated Fibrin gels deliver contents into the site of injury as the polymer and covalent bonds binding the bioactive factors are degraded. Previous studies using PEG-fib as a bioactive factor delivery agent, in myocardial infarction models, showed improved left ventricular function following treatment (Zhang et al., 2007, Zhang et al., 2008). Additionally a subsequent study looking at the role of IGF release into tourniquet induced ischemia/reperfusion (I/R) found that while most of the IGF was released within the first 24 hr after injection, IGF continued to be released at

physiologically relevant quantities 96 hrs post injection; an effect that significantly improved functional and morphological recovery of the lateral gastrocnemius (LGAS) (Hammers et al., 2011). The role PEG-fib has in bioactive factor delivery makes it an attractive option for VML treatment.

Of great importance is the role of motoneurons in the regeneration and long term survival of muscle fibers. Without continued stimulation muscle fibers initially recover but cannot sustain regeneration and functional impairments arise (Borisov et al., 2001, Borisov et al, 2005). The morphology of muscle is directly influenced by activation and innervation of the nerve as seen by cross-innervation studies (Nehrer-Tairych, et al., 2000). Neurotization of the ECM and associated myofibers is likely to enhance regeneration. An increase in ectopic motor endplates distal to native end plates is seen due to neurotization of distal zones, indicating the importance of implant location in end plate formation and reinnervation. This study however did not measure functional output to analyze differences in location and resulting end plate morphology (Payne and Brushart, 1997). Neural growth factors and brain derived growth factors, known as neurotrophins, are secreted by peripheral nerves and aid the regulation of axonal growth, survival and death. Studies in which neurotrophic KO mice are used, exhibit decreased muscle development and function, or postnatal lethality, indicating an important physiological role of neurotrophic factors in muscle regulation (Clow and Jasmin, 2010). Nerve growth factor (NGF) has been shown to be expressed in regenerating myofibers and when engineered to be expressed in stem cells dystrophic mice show improvements in regeneration. On the other hand, brain derived neurotrophic factor (BDNF) plays a key

role in satellite cell function and muscle regeneration (Clow and Jasmin, 2010, Lavasani et al., 2006). The positive effect seen with neurotization of muscle tissue alone, or in concert with other bioactive factors, on muscle repair make a strong case for the use of a combined treatment as a therapeutic modality for VML injury.

Therefore, this study aimed to investigate the effects of a combined treatment in the functional and morphological recovery of the lateral gastrocnemius muscle, 56 days post VML injury using plantar nerve relocation on an extracellular matrix seeded with mesenchymal stem cells in a PEGylated fibrin gel.

REVIEW OF LITERATURE

Skeletal Muscle Overview

Skeletal muscle, made up of individual multinucleated myofibers that bundle together and are surrounded by the endomysium, perimysium, and lastly the epimysium, constitutes approximately 45% of one's body weight in the normal population and is of great importance to locomotion (Huard et al., 2002, Juhas and Bursac, 2013). It is composed of many structural and functional proteins and within its framework, it contains vascular and neuronal processes that aid in the muscle's functional propensity. Its capacity for regeneration and self repair has been extensively studied. Skeletal muscle injuries can occur due to three direct traumatic causes: contusion, strain, and laceration or indirect causes such ischemia and neurodegeneration (Jarvinen et al., 2005, Huard et al., 2002). Unlike other tissues in the body, skeletal muscle has a great propensity for self repair, even with aging, unless involved in traumatic injuries. Muscle begins regeneration promptly following severe soft tissue damage but depending on the severity of injury can be hindered due to scar tissue deposition within the site of injury. The process of self repair in skeletal muscle can be broken down into three distinct phases.

Destruction phase

The destruction phase following skeletal muscle injuries is characterized by lesions/rupture of the ECM, sarcoplasmic reticulum, and its associated myofibers, this damage then results in necrosis of those injured myofibers (Jarvinen et al., 2005). The ruptures associated with injury cause an influx of calcium into the tissue which then leads

to subsequent activation of proteases. Furthermore, necrosis is characterized by two distinct steps: a rapid onset in which plasmalemmal and myonuclear losses are seen, and then a gradual necrosis that leads to contractile material and cellular organelle loss (Karpati and Molnar, 2008). However, in order to prevent the propagation of necrosis along the entire muscle fiber, skeletal muscle forms a contraction band that acts as a sealant of the plasma membrane through lysosomal vesicle deposits, in order to allow the muscle fiber to repair the plasma membrane and its associated defect area (Jarvinen et al., 2005, Jarvinen et al., 2007, Jarvinen et al., 2008). In addition to the injury suffered by the plasma membrane of skeletal muscle, ruptures also occur in the associated blood vessels which lead to the release and leukocytes to the injured area. The first inflammatory cells to respond are a type of phagocitotic white blood cell, known as neutrophils, which clear the site of injury from necrotic tissue and debris through oxidative and proteolytic modification (Tidball, 2005). A second type of phagocitotic white blood cell, known as a macrophage, then follows to continue clearance of debris. Tissue macrophages and fibroblasts within the injury then become activated, and begin the release of chemokines, such as TNFα and IL-6, as well as MCP-1 which attract circulating inflammatory cells (Juhas and Bursac, 2013, Jarvinen et al., 2005, Jarvinen et al, 2008, Schiaffano and Partridge, 2008, Tidball, 2005, Chazaud et al., 2008, Charge and Rudnicki, 2004). Once inflammation and necrosis removal has slowed down the macrophage profile within the muscle is said to change from M1 phagocitotic macrophages to anti-inflammatory M2 within 24 -48 hrs post injury (Rigamonti et al., 2014, Arnold et al., 2007, Chazaud et al., 2008). M2 macrophages play a role in the decrease of inflammation and switching the

environment towards one conductive to regeneration through their secretion of TGF-β, IGF1, and IL-10 (Rigamonti et al., 2014, Tidball, 2004). Despite the differences in secretion and function between the two populations of macrophages, ultimately both populations act on satellite cells to first activate and proliferate, and then to differentiate (Rigamonti et al., 2014, Tidball, 2005, Jarvinen et al., 2005). Tissue necrosis and inflammation play a key role in muscle regeneration due to their role in chemokine release and without them regeneration is hindered.

Repair phase:

Although thought to be a distinct phase, the repair phase begins during the degeneration phase due the effects macrophages have on satellite cell activation, proliferation, and differentiation. The repair phase is characterized by two simultaneous processes: muscle fiber regeneration and scar tissue formation (Jarvinen et al., 2005). Muscle fiber regeneration begins with the activation, proliferation, migration to the site of injury, and then differentiation of pax 7+ satellite cells into myoblasts, through expression of MyoD (Juhas and Bursac, 2013, Wang and Rudnicki, 2012, Charge et al., 2004, Collins and Partridge, 2005). Activation of satellite cells is characterized by nuclear enlargement, nucleus to cytoplasmic mass increases, and upregulation of DNA synthesis (reviewed in Carlson and Faulkner, 1983). Studies looking at satellite cell activation have shown that the autocrine splice variant produced by muscle, mechano growth factor, is responsible for the early activation of satellite cells while insulin growth factor is responsible for the maintained activation and proliferation, as IGF-1 expression

peaks at 11 days post injury (Hill et al., 2003). Once committed to a myogenic lineage, satellite cells express myogenin, continue myoblast proliferation, followed by fusion to damaged tissue or each other. Satellite cell engraftment into muscle tissue has been extensively studied in many animal models and it has been shown that ablating the satellite population of a mouse and implanting β-gal satellite cells generates myofibers in which over 50% of the population are β-gal + (Collins et al., 2005). Additionally, it has been shown that as few as 7 satellite cells can produce more than 10 times the amount of myofibers per satellite cell (Collins et al., 2005). With age the capacity for self renewal and repair of skeletal muscle diminishes, due in part to impaired Notch and Delta signaling. Parabiosis studies with old and young mice have shown the importance of satellite cell activation through their environment. In these studies old mice matched with young environments saw enhanced muscle regeneration in part due to an upregulation of Delta in the old mice (Conboy et al., 2005). These studies show the significance in the role that niche regulation plays on satellite cell activation and the subsequent role that these cells have on regeneration.

While satellite cells are the primary contributors to new nuclei in the muscle, different populations of cells have been shown to also play a role in the regeneration of skeletal muscle. Notable are the resident muscle-derived stem cells and the bone marrow stem cells (Charge, 2004, Juhas and Bursac, 2013). These cells travel to the site of injury from locations distant to the injury and muscle and either directly contribute to regeneration through myonuclei donation or through secretion of growth factors that alter surrounding cells and contribute to a changing niche environment (Quintero et al., 2009,

Sun et al., 2009, Tedesco et al., 2010). The exact mechanism by which they contribute to muscle regeneration is still relatively unknown, but it is hypothesized that these cells may contribute to the repopulation of the satellite cell pool (Kuang et al., 2008, Usas and Huard, 2007). Additionally, the tolerance displayed by muscle derived cells to manipulation ex-vivo, as well as their multipotency, make them viable options for regenerative purposes (Usas and Huard, 2007, Lavasani et al., 2006). Thanks to cellular contribution by these groups of stem cells the repair phase is characterized by the regeneration of myofiber, endothelial, and nerve tissue.

Following injury, ruptured fibers are filled with a hematoma and blood-derived cells infiltrate the site of injury, such as fibrin and fibronectin which form granulation tissue (Jarvinen et al., 2005). This tissue acts as a way to bridge the gap between the myofiber stumps and to provide tensile strength within the tissue while the fibroblasts restore the ECM integrity (Jarvinen et al., 2005). Unfortunately, if injury to skeletal muscle is significantly severe scar tissue formation can hinder regeneration.

Remodeling Phase

In the remodeling phase after injury, maturation of myofibers are witnessed by the migration of nuclei from a central position to the periphery. This transition causes the nuclei to then form attachments to the extracellular matrix. Maturation of myofibers and scar tissue remodeling continues via myofiber protrusion through the scar until function is restored (Jarvinen et al., 2005, Kaairiainen et al., 2000). This remodeling phase is hindered when damage is significant and the fibrotic scar tissue is too large to overcome,

an effect that is largely seen in trauma related injuries, such as VML injury. The resulting tissue is then left devoid of myofibers, nerve, and expresses large functional deficits. In this study we examined neurotization and stem cell administration as therapeutic strategies for VML injury, to counteract the deficits seen in regeneration with in this injury model.

Skeletal Muscle Trauma

Penetrating traumatic lesions to the extremities comprise a large population of injuries in the battlefield by military personnel, those going through surgical ablation and motor vehicle accidents within the civilian population. In the case of battlefield injuries, over half of the injuries in Operation Iraqi freedom and Operation Enduring Freedom were skeletal muscle injuries (Owens et al., 2006). Injury is quite extensive and comprises damage to the skeletal muscle, bone, nerve, and vascular system within the tissue. Primary care to the injuries focuses on bone repair and prevention of infection, often leaving the tissue untreated. Patients incur significant muscle loss, known as volumetric muscle loss, lack of adequate vascularization, and improper nerve stimulation which result in significant functional deficits, as well as cosmetic deformities, and associated mental distress. Volumetric muscle loss injuries display increased scar tissue deposition and reduced regenerative capabilities. If the muscle is left untreated, myofibers are unable to bridge the gap by their own repair process and a major deficit within the tissue is observed, which is then followed by deposition of dense scar tissue rendering it impossible for penetration by myofibers and blood vessels (Merritt et al.,

2010, Terada et al., 2002). Limb salvage for VML injuries does not restore function in the tissue and currently clinical treatments use function free muscle transplants, which risk donor site morbidity and infection, and bracing to further treat the injury (Grogan and Hsu, 2011). In a study that looked at deployment following limb salvage, the authors reported four patients requesting late amputation due to debilitating functional loss (Patzkowski et al., 2012). Furthermore, a study looking at medical costs for treatment of VML injuries by the department of defense estimates over a half a billion dollars for initial hospital treatment and close to two billion dollars in disability benefits (Masani et al., 2009). Therefore, it is imperative that treatments should focus on enhancing myofiber repair/regeneration within an appropriate scaffold which is conductive to increased regeneration, in order to increase function.

Extracellular Matrix as a Conduit for Regeneration

In recent years, due to autologous tissue grafts leading to donor site morbidity and hindered functional regeneration, bioengineering strategies have searched for alternatives to increase regeneration of tissue. Tissue engineering has looked at a number of nonautologous/acellular grafts, natural-based materials, and synthetic materials to aid in both skeletal muscle and nerve regeneration (Schmidt and Baier Leach, 2003). Xenogenic and synthetic materials have been attractive alternatives to tissue grafts due to their reproducibility, availability, and patient tissue exclusion. Despite their attractiveness in tissue engineering, these materials possess risk of disease transmission, elicit

immunogenic responses, and in certain cases, impermeable materials do not support large defect regeneration (Schmidt and Baier Leach, 2003, Meintjes et al., 2011). Thus focus should be placed on natural-based materials like the extracellular matrix for tissue regeneration. The extracellular matrix is a three-dimensional structure that contains proteins and carbohydrates and is responsible for aiding in cell proliferation, differentiation, and migration. The ECM is present in all tissues of the body and aids in function by allowing transduction of mechanical force down the ECM, provides structural support, and it provides the framework for tissue growth, communication, and cellular infiltration (Gonzalez-Perez et al., 2013, Badylak, 2007, Brown et al., 2009). Studies have shown pliability of the ECM to have an effect on MSC, with soft matrices enhancing MSC regeneration of endothelial tissue (Wingate et al., 2013). Individual components of the ECM have been isolated and studied but have shown differences in response. Of the ECM proteins, collagen, laminin, fibronectin, and integrin have been extensively studied (Singhal and Martin, 2011, Gonzalez-Perez et al., 2013, Badylak, 2008, Hinds et al., 2011). Laminin and nerve growth factor seeded on an agarose hydrogel, show dorsal root ganglia neurite extension comparable to collagen matrices experiments (Yu et al., 1999). Collagen and fibronectin composition of hydrogels have shown to increase contractility of tissue (Hinds et al., 2011) and Schwann cell proliferation (Armstrong et al., 2007). On the other hand, tissue exhibiting deficiencies in any of these components exhibit improper function and formation, notably those with laminin β2 deficiencies show decreased Schwann cell migration, while those lacking integrin β1 lack innervation by the motor neuron and show impaired myoblast fusion

(Singhal and Martin, 2011, Schwander et al., 2003, Schwander et al., 2004). Additionally, diseases in which ECM proteins are altered or defective show increased muscle cycling between regenerative and degenerative states. All together this contributes to the need for complete ECM use for proper tissue regeneration.

Currently there are many commercially available scaffolds for use from various tissues including bovine, porcine, and human (Brown and Badylak, 2014, Badylak et al., 2008). The most researched ECM for tissue regeneration is the xenogenic porcine ECM of the SIS and have been used in volumetric muscle loss models, as well as in the reconstruction of urinary tract, skin, and arteries (Badylak, 2003). The SIS scaffold is constructed by vacuum pressing several layers of the tissue together (Badylak, 2007). SIS scaffolds have been used in comparative studies and have been shown to increase cellular response (Wolf et al., 2012, Badylak and Gilbert, 2008). Additionally, the use of SIS in a clinical application to treat VML has shown an increase in function following reparative treatment (Mase et al., 2010). Of great importance in regenerative therapies have been studies which have shown that non cross-linked ECMs have increased neovascularization, cellular infiltration and substantial tissue remodeling (Wolf et al., 2012, Badylak, 2004). However, tissue ECM must first be decellularized for implantation as cellular remnants produce an immunogenic response characterized largely by type one macrophages, a characteristic that greatly reduces regeneration capacity of the tissue. Studies have shown that acellular grafts are more conducive to regeneration, in part due to the recruitment of type two macrophages through degradation, by plasminogen (Sicari

et al., 2014, Brown et al., 2009), and subsequent remodeling, which leads to chemoattractant release and recruitment of progenitor cells to the tissue (Badylak et al., 2009, Badylak and Gilbert, 2008, Badylak, 2008, Badylak et al., 2001). Furthermore, comparative studies have shown increased perivascular stem cell growth in muscle derived ECM scaffolds compared to SIS-ECM a characteristic attributed to growth factors and attachment proteins specific to muscle derived ECM (Wolf et al., 2012). After injury, macrophages and satellite cells secrete matrixmetalloproteinase (MMP) which causes bound growth factors, such as vascular endothelial growth factor (VEGF) and hepatocyte growth factor (HGF), to be released into the environment, which in turn signals migration of progenitor cells to the area (Lolmede et al., 2009, Tatsumi, 2010). A study looking at C_2C_{12} myoblasts seeded on decellularized, muscle derived ECM extract coated surfaces saw an increase in proliferation and differentiation of myoblasts (Stern et al., 2009) while implantation of C_2C_{12} myoblasts into the ECM increased contractility following incubation in differentiation medium (Borschel et al., 2004). Thusly, tissue-specific ECMs are emerging as an attractive alternative to xenogenic tissue in VML injuries due to specificity of growth factors and proteins within the ECM and their conduciveness to regeneration of the tissue.

Work within our laboratory on muscle derived ECM in volumetric muscle loss injuries has shown promising results. Experiments have shown that implantation alone does not restore function; yet seeding with mesenchymal stem cells produces an increase in contractility of the tissue (Merritt et al., 2010). However, despite improved

contractility histological analysis showed an area devoid of blood vessels and myofibers. A subsequent unpublished study showed significant functional recovery and myofiber regeneration, in the previously hypoxic core, 42 days post injury following neurotization (Tierney et al., 2010). Another study within our lab delivered MSCs using a PEGylated fibrin gel 56 days post injury, in a larger defect area, showed marked improvements as well (Merscham-Banda et al, 2012). Therefore, a combination of treatments is likely prospect for future studies of VML.

Mesenchymal Stem Cells in Muscle Repair

Stem cells have long been an attractive tool for cellular and regenerative therapies; however, recent studies have focused on isolation of stem cells from a variety of sources, including adult tissue. Mesenchymal stem cells, first characterized by Freidenstein in 1974, have been shown to give rise to osteocytes, adipocytes, and chondrocytes *in vitro* and are an attractive tool in cell therapy due to their accessibility, adherence in culture, and proliferative capabilities, as well as their transdifferentiative abilities due to spontaneous cell fusion (Pittenger et al., 1999, Keilhoff et al., 2006, Woodbury et al., 2002, Terada et al., 2002, Ripoll and Bunnell, 2009). Despite their ease of acquisition through bone marrow aspiration, these cells have been difficult to characterize due to presence of intermittent surface marker presentation, such as CD 34 during certain conditions, and the same markers in both stem populations and non stem populations (Pittenger et al., 1999, Pittenger and Martin, 2004). Initially, following

isolation the cell population is heterogenous but following multiple weeks of expansion the population becomes more homogenous (Pittenger and Martin, 2004, Prockop, 1997).

Mesenchymal stem cells are an attractive treatment model for their potential incorporation into muscle tissue. Interestingly, following a bone marrow transplant and subsequent irradiation treatment of satellite cells in animal models, green fluorescent protein tagged (GFP+) MSCs have been shown to mobilize and occupy the satellite cell niche, indicating a large role in MSC repopulation of another stem cell population (LaBarge and Blau, 2002, Collins et al. 2005, Dezawa et al., 2005). Additionally, following exercise induced stress a 20 fold GFP+ increase is seen in myofibers, indicating incorporation of these MSC first into the satellite cell niche and then into myofibers. Other studies have looked at intravenous delivery of MSCs and have been met with promising results, indicating that circulating bone marrow cells have a large capacity to aid in repair of tissue as seen by parabiosis studies in which incorporation of MSC are seen following damage (Palermo et al., 2005). Following intravenous administration of MSC in irradiated *mdx* mice, hematopoietic cells were shown to be donor-derived at 5 weeks, and after 12 weeks as many as 10 percent of myofibers showed recovered expression of dystrophin (Gussoni et al, 1999). In a similar study CD 271+ MSCs were intravenously injected in canine model of Duchenne muscular dystrophy and saw upregulation of dystrophin, 12 weeks post treatment (Nitahara-Kasahara et al., 2012). Intravenous injections of human mesenchymal stem cells have also shown to improve heart function following myocardial infarction (Yeghiazarians et al., 2009, Lee et al., 2009). The cardioprotective effect witnessed in stem cell transplantation, has been

characterized by the secretion of anti-inflammatory, TNF-α protein 6 (TSG-6), as well several growth factors, including vascular endothelial growth factor (VEGF), nerve growth factor beta (NGF-β), brain-derived neurotrophic factor (BDNF), and insulin-growth factor (IGF) (Lee et al., 2009, Qu et al., 2007, Sadat et al, 2007). Stem cell therapies have also been useful in peripheral nerve repair studies in which intravenous injections of MSC following nerve crush injuries showed improvements in functional measures 7 days post treatment and maintained through 21 days. Additionally within this study, histological measures showed increased axonal regeneration (Matthes et al., 2013). Despite increased evidence of the beneficial role of MSCs in regenerative treatments, debate and uncertainty persists on the mechanisms for functional and morphological improvements following MSC treatment (Prockop et al., 2003). Taken together these studies show an immense potential for regenerative therapy.

Stem Cell Delivery Using a PEGylated Fibrin Gel

Research in the field of tissue engineering has experimented with natural materials and synthetic materials for drug and biofactor delivery due to the short half-life of most growth factors. Similar to the way ECM provides a three dimensional environment for proliferation and differentiation, growth, and attachment of cells, synthetic materials such as matrigel and hydrogels are able to mimic these characteristics as well. Matrigel experiments for MSC delivery found both angiogenesis and vasculogenesis two weeks post implantation compared to matrigel only, explained by depleted oxygen tension in the Matrigel implant which causes and upregulation of VEGF

production by MSCs (Al-Khaldi et al., 2003). Drug and biofactor delivery is being improved through the synthesis of biomaterials that use cytokine affinity to fibrin in order to contain these biofactors within the matrix. Another biofactor delivery tool is Poly-(ethylene glycol) (PEG), a nontoxic hydrophilic polymer, that in a process called PEGylation, is conjugated to fibrinogen and thrombin from human plasma. Studies looking at the effect of these biomaterials, have found that PEG aids in the prevention of nerve cell rupture following spinal cord injury by sealing damaged membranes, while delivery of fibrin alone via subcutaneous administration stimulates capillary ingrowth (reviewed in Nisbet et al., 2008, reviewed in Zhang and Suggs, 2007). Due to their individual effects, researchers have thus looked at the effects of combining PEG and fibrin in order to covalently localize factors within the matrix, these factors are then released via degradation of the matrix by serine proteases and matrix metalloproteinases (MMP) (reviewed in Zhang and Suggs, 2007, Zhang et al., 2008). Biofactor delivery of IGF, using a PEGylated-fibrin gel, in an Ischemia/reperfusion injury model greatly improved functional recovery 4 days post injury, likely due to significant continued release of IGF 96 hrs post injection (Hammers et al., 2012). In a previous experiment, delivery of MSCs and HGF using PEGylated Fibrin gel, following myocardial infarction, showed increased cell survival and cell clusters within the heart, as well as improvements in left ventricular function (Zhang et al., 2008,). Additionally, studies within that same lab have studied dual release of platelet derived growth factor bb (PDGF-BB) and transforming growth factor β-1 (TGF β-1), *in vitro.* The study showed a fast release of PDGF-BB and a slow release of TGF β-1(Drinnan et al., 2010). Therefore, a systematic

and slow release of MSC via PEGylated fibrin degradation could promote angiogenesis in a volumetric muscle loss model and thus increase function.

Reinnervation and Vascularization of the ECM

Reinnervation following skeletal muscle injury plays a crucial role in the regenerating capabilities of the muscle. Reinnervation of new myofibers is critical in a volumetric muscle loss injury model in order to express mature myofiber phenotypes and increase functional capacity. Skeletal muscle that has been denervated continues the path of regeneration despite lack of innervation, but if the neuromuscular junctions fail to be reinnervated, atrophy and tissue necrosis ensue (Jarvinen et al., 2005). Ensuing atrophy of the muscle occurs at different rates, with fast muscle fibers displaying atrophy at faster rates than slow muscle fibers. Atrophy is then accompanied by structural remodeling, as well as loss of mitochondria, actin, and myosin (Borisov et al., 2001). Furthermore, following denervation, myogenesis occurs through satellite activation but this process is haulted within five to seven months post denervation due to satellite cell depletion, a process that affects differentiation of muscle fibers (Borisov et al, 2005). Due to the adverse effects seen following denervation, it is critical that new myofibers be reinnervated following VML injury. Studies involving neurotization in the rat soleus show no change in reinnervation of native end plates as result of the location of the nerve implant, however an increase in ectopic to native innervation ratio is witnessed with a distal nerve implantation (Payne and Brushart, 1997). Despite promising motor end plate formation that could aid in sustaining survival and function of myofibers, the study did

not determine functional capabilities of the tissue. However, when direct contact is formed between the nerve and a motor end plate, successful reinnervation is witnessed (Bixby and Van Essen, 1979). Successful innervation of tissue and regeneration of nerves is dependent on glial cells known as Schwann cells. Schwann cells become proliferative and activated to secrete and produce cytokines and neurotrophic factors that play an important role in axon guidance (Shimizu et al., 2007). Following dennervation, reinnervation by axons is dependent on previous Schwann cell tubes, as well as newly formed Schwann cell processes leading to end plates, a process that is limited by Schwann extension (Son and Thompson, 1995, 1995b, Son et al., 1996, Love and Thompson, 1998). However, axonal extensions, following reinnervation, were withdrawn if not directly led by Schwann cell process (Kang et al., 2003). A study examining the role of Schwann cells and axons following neurotization of the soleus, witnessed Schwann cell and axon migration to the soleus from the cut end of the transplanted nerve, a process that occcurred regardless of concurrent migration by axons (Son and Thompson, 1995, 1995b). Despite the critical role Schwann cells play in axonal guidance, the presence of motoneurons is also paramount to Schwann cell viability. Motoneurons act on terminal Schwann cells, via the secretion of glial growth factor, a neuregulin that activates proliferation, migration, and survival (Trachtenberg and Thompson, 1996, 1997, Kopp et al., 1997). Neuregulin, additionally acts on muscle by binding tyrosine kinase receptors of the epidermal growth factor family (Erb). The effects of neuregulin on myoblasts were observed following treatment of human primary myoblasts. Human primary myoblasts treated with neuregulin expressed increases in

acetylcholine receptors, increases in the thrombospondin-1 gene, that regulates proliferation, migration, and apoptosis, as well as increases in myosin heavy chains associated with muscle spindle fibers (Jacobson et al., 2004). Other studies have looked at the role of several neurotrophic factors on skeletal muscle regeneration and neurite extension. In an mdx model, muscle-derived stem cells treated with nerve growth factors (NGF) showed enhanced muscle regeneration, and similarly NGF treated laminin scaffolds showed increased dorsal root ganglia, neurite extension (Lavasani et al., 2006, Yu et al., 1999). Lastly, to examine the role brain-derived neurotrophic factor (BDNF) plays in muscle regeneration, the effects of BDNF were observed in BDNF depleted mice which displayed decreased Pax 7+, satellite cell expression, as well as impaired regeneration, characteristics that were rescued with exogenous BDNF treatment (Clow and Jasmin, 2010). These studies highlight the importance of the interaction between muscle, nerve and terminal Schwann cells in the maintenance of the neuromuscular junction.

In a study using stem cell therapy, SK-34 muscle derived stem cells were implanted following injury in the mouse tibialis anterior. This study found increased detection of donor-derived myofibers, blood vessels, and nerves, characteristics that were closely associated with increased mass and function of the tissue (Tamaki et al., 2005). The close association between these three tissue types and function reveals a need for a therapy that involves increases in regeneration of myofibers and nerves, and increased blood vessel density within the ECM construct. A previous study looking at the role of neurotization by the femoral nerve in a three dimensional construct showed a 5 fold

improvement in function as well as blood vessel formation within the construct (Dhawan et al., 2007). In a later study, within our lab, looking at the role of neurotization in a VML injury, it was observed that neurotization significantly increases blood vessel density, tissue morphology, and function following MSC treatment and peroneal nerve transplantation (Tierney et al, 2010, unpublished). The close association between nerves and blood vessels is characterized by the role Netrins, Slits, and Semaphorins have on both neural guidance and blood vessel navigation (Autiero et al., 2005). The increase in blood vessel density in the previously hypoxic ECM core following neurotization, displays a strong link between vascularization, innervations, and regeneration.

SIGNIFICANCE

Approximately, 1.3 million men and women in the United States are on active duty in our armed forces according to the US Department of Defense. Musculoskeletal extremity injuries have been reported to comprise approximately 50% of all combat wounds with most being from remnants of exploding grenades and missiles (Belmont et al., 2010). The repercussions of such injuries are profound, often causing VML injuries, and subsequent functional deficits (Sarathy et al., 2011, Unpublished). In cases of extensive traumatic injury, amputation of the injured extremity is needed (Zouris et al. 2006). These injuries not only can cause severe physical abnormalities, often leaving gaps in areas where muscle regeneration is hindered often associated impeding function, but emotional distress over the aesthetic unpleasantness of physical abnormalities. The emotional distress suffered by veterans is not limited to only military populations but includes civilian populations incurring traumatic injuries from surgical ablations, severe motor vehicle accidents, and degenerative diseases. VML injuries in soldiers cause the greatest number of disabilities and the greatest amount of disability benefit costs (Grogan and Hsu, 2011). The increasing severity of injury during combat due to IEDs and the subsequent emotional distress associated with functional and aesthetic impairments in military and civilian populations due to traumatic injury attest to the importance of finding better therapeutic modalities to increase muscle regeneration and function following severe muscular injury.

This study aims to assess the functional recovery of major muscular injuries, such as those suffered in combat, degenerative disease, and by medical procedures that result

in a VML injury. The current study is to determine the influence of neurotization of an ECM and stem cell administration via PEGylated fibrin gel on muscle regeneration. Previous work has led to our model of using a decellularized extracellular matrix (ECM) as a biological scaffold to support and guide myofiber in-growth in the defect site, albeit some major hindrances have been seen, such as the hypoxic core seen at 42 days recovery time (Merritt et. al, 2010). Other studies have shown ECM degradation to promote the recruitment of Schwann cells to the injury site (Agrawal et al., 2009). Preliminary data within our lab demonstrates that biofactor delivery via PEGylated Fibrin gel significantly improves function and structure of the injured muscle (Hammers et al., 2012). By looking at neurotization, the effects of time dependent stem cell release, and extended recovery time we will gain a better understanding of how various therapeutic modalities can increase regeneration which can have a clinical impact in the treatment of civilian and military populations suffering from a volumetric muscle loss.

METHODS

ANIMALS

Male Sprague Dawley transgenic Rats for YFP under the S100 promoter (Wesley Thompson's Laboratory, Texas A&M/ University of Texas-Austin) age 3-7 months were used in this study. Animals were housed on a 12 hour light/dark cycle and allowed access to food and water, *ad-libitum*. Rats were randomly assigned to 6 groups (n=5-6). Animals in the study were treated in compliance with the ethical guidelines Institutional Animal Care and Use Committee (IACUC).

EXTRACELLULAR MATRIX DECELLULARIZATION

Extracellular matrices were isolated from donor Sprague Dawley rats and decellularized using a protocol from our laboratory. Donor tissue was harvested and placed in 4% deionized water (dH_2O) for 24 hours in order to induce cell swelling and consequent rupture. Donor ECM was then placed in a glycerol (Fisher; Pittsburgh, PA), sodium dodecyl sulfate (SDS) (Sigma-Aldrich; St. Louis, MO), disodium ethylenediaminetetraacetate dehydrate (EDTA) (Bio-Rad Laboratories; Hercules, CA), and deoxycholic acid (Fisher; Pittsburgh, PA), solution for 24 hours to prepare for storage and placed in the freezer or placed in a Tris base (Fisher; Pittsburgh, PA), Glycine (Fisher; Pittsburgh, PA), and SDS (Sigma-Aldrich; St. Louis, MO) and run on an electrophoresis machine. The tissues were run in the electrophoresis machine with a constant voltage of 15V for six hours and then placed in SDS overnight. The electrophoresis process was repeated until all cellular material was removed. The ECM

was placed in DH_2O for twenty-four hours followed by placement in sterile phosphate buffered saline (PBS) (Invitrogen; Carlsbad, CA) over night in order to remove remaining SDS from the matrix. Next the ECM was placed in ethanol for four hours, followed by multiple rinses in PBS. Lastly, the ECM was placed in sterile PBS with 1% antibiotic-antimycotic (AA) (Sigma-Aldrich;St. Louis, MO) and exposed to ultraviolet light for at least 12 hours. Tissue was then stored at 4˚C until ready for use in VML treatment.

MSC ISOLATION AND CULTURE

Bone marrow was obtained via surgical removal of the femur and tibia of Sprague Dawley rats. The shaft of the femur and tibia were flushed with Dulbecco's modified eagle's medium (DMEM) (Invitrogen; Carlsbad, CA), 10% fetal bovine serum (FBS) (Invitrogen;Carlsbad, CA), and 1% AA media solution using an 18G needle. Cells were disaggregated via gentle pipetting then centrifuged at 1000g, at 4˚C for 5 minutes. The resulting pellet was resuspended in the aforementioned solution and on a culture flask and incubated overnight at 37˚C and 5% CO_2. After 24 hours of incubation, the non-adherent fraction was removed, centrifuged, and replated. Cells were maintained at 37°C and 5% CO2 and passaged as the cells reached 70% confluency. Once cells reached desired confluency, cells were removed from the flask using 0.25% trypsin in 1mM EDTA, then centrifuged and replated. Cells were then implanted once they reached passages 3-7. Animals receiving MSC injections were injected 1.5-2 billion cells in 25µl of PBS.

SURGICAL PROCEDURES

Prior to surgery, animals were randomly placed in one of six experimental groups: implantation of the ECM (Saline), implantation of the ECM followed by PEG injection(PEG), implantation of the ECM followed by PEG and BMSC injection (PEGMSC), implantation of the ECM followed by relocation of the plantar nerve (N), implantation of the ECM followed by plantar nerve relocation and PEG injection (NervePEG) and implantation of the ECM followed by plantar nerve relocation followed by PEG and MSC injection(NERVEPEGMSC). All surgery was performed under aseptic conditions while rats were anesthetized using 2% Isoflurane.

An approximately 2.0 cm incision was made into the skin at the lateral side of the lower leg, parallel to the tibia. The lateral portion of the LGAS was exposed by separating the biceps femoris from the tibia (Figure 1A). Following isolation from the soleus, a metal plate was used to keep separation between the soleus and LGAS. Two #9 scalpel blades separated by a spacer were then used for removal of an approximately 1.0 x 1.0 cm full thickness piece of the lateral gastrocnemius (LGAS) distal to the neuromuscular junction (Figure 1B). The excised muscle was weighed and recorded. The defect area was immediately replaced with a homologous, decellularized, extracellular matrix (ECM) of the same dimensions and sutured with nonabsorbable 5-0 polyprolene (5-0 prolene; Ethicon) sutures (Figure 1C). A modified Kessler stitch with simple interrupted sutures on all 3 borders was utilized to secure the ECM into the defect area and serve as markers for later analysis (Kragh et al. 2005). The biceps femoris was sutured closed using simple interrupted polyprolene sutures (5-0 prolene; Ethicon). The

skin was closed using a simple interrupted suture (5-0 prolene; Ethicon) with the knot tied underneath the skin to prevent the animal from opening the incision.

NERVE RELOCATION

During the initial defect creation, an approximately 1.0 cm incision was made on the medial side of the lower leg parallel to the tibia. The medial plantar nerve was isolated from its lateral counterpart and surrounding tissue and was denervated as distally as possible. The cut nerve end was redirected through the anterior and posterior compartments to the defect area (Figure 1D). Perpendicularly oriented myofibers of the LGAS and the defected area, the nerve was secured to the ECM with one non-absorbable polypropylene 9-0 suture. Following relocation, wounds were sutured as aforementioned.

PEGYLATED FIBRINOGEN PREPARATION

Succinimidylglutarate bi-functional polyethylene glycol (3400Da, NOF America; White Plains, NY) was added to human fibrinogen (80mg/ml, in PBS pH 7.6, Sigma; St. Louis, MO) at a molar ratio of 10:1 and incubated at 37°C for forty-five minutes. PEGylated fibrinogen underwent gelation by adding an equal volume solution of thrombin (25U/ml in 40mM calcium chloride, Sigma; St. Louis MO).

INJECTIONS

After seven days of recovery following initial injury, the animals were anesthetized using 2% isoflurane. The original skin incision was reopened, and the

LGAS was exposed to visualize the ECM. The ECM was injected in 4-6 locations using a 26-gauge needle with 200µl of saline (SAL), 200µl of PEGylated fibrin (PEG), or 200µl of mesenchymal stem cells seeded in PEGylated fibrin (PEG+MSCs (Figure 1E). After injection, the wounds were sutured as aforementioned.

FUNCTIONAL ANALYSIS

Following 56 days recovery, *in situ* measurements were performed on both the experimental and the contralateral (internal control) leg. Animals were anesthetized as previously mentioned. An incision approximately 2 cm long was created parallel to the femur in order to expose the sciatic nerve. Once isolated from connective tissue and fat deposition, the sciatic nerve was cut as proximal to the hip as possible. A longitudinal skin incision was made along the posterior portion of the lower leg from the calcaneus to the popliteal region. The skin was separated from the biceps femoris, and a similar incision was made along the biceps femoris from the calcaneus to the popliteal region. The biceps femoris, soleus, and plantaris were separated from the gastrocnemius. Following separation of the LGAS, the medial GAS was dennervated to ensure force production isolated to the LGAS. The calcaneus was detached and the Achilles tendon was attached to a dual mode servomotor muscle lever system (model 310-B, Aurora Scientific, ON, Canada). Electrodes were placed on the sciatic nerve, and the muscle was stimulated to elicit maximal isometric tetanic contractions using a stimulator (Model 2100; A-M Systems, Carlsborg, WA). The muscle was kept wet in mineral oil and the temperature was maintained between 36.5°C and 37.5°C with a radiant heat lamp. The

muscle length was adjusted to optimal muscle length with a micrometer. Peak tetanic tension was stimulated at 150 Hz and the minimum voltage necessary to elicit maximal contraction. After each contraction, the muscle was allowed to rest for 2 minutes. Total force, cross sectional area, and specific tension were determined. Following termination of functional measures, muscles were excised, weighed, and encapsulated by OCT and frozen in liquid nitrogen cooled isopentane. Tissues were stored in -80˚C for future histological and immunohistological analysis.

HISTOLOGICAL ANALYSIS

Following functional analysis, the experimental LGAS was removed, cleaned of external connective tissue and excess fat, weighed, and frozen in liquid nitrogen cooled isopentane. Series of 5 μm sections were taken perpendicular to myofiber orientation and within the Top, Middle, and Bottom regions of the implanted ECM using a Leica CM1900 cryostat microtome (Leica Microsystems; Wetzlar, Germany) at -20°C. Following sectioning slides were immediately placed in acetone for 5 minutes. To identify myofibers, nuclei, and collagen, Hematoxylin and eosin (Sigma-Aldrich; St. Louis, MO) staining was performed.

IMMUNOHISTOCHEMISTRY ANALYSIS

In preparation for immunofluorescent identification, sections were placed in acetone for 10 minutes, followed by 3- 5 minute washes of PBS. Sections were blocked

with 10% normal donkey serum in PBS. All of the following materials were purchased from Santa Cruz Biotechnologies, Santa Cruz, CA unless otherwise stated. Sections were first incubated with primary antibodies, in PBS containing 5% bovine serum albumin (BSA), against PECAM (2:100, goat polyclonal), rinsed with PBS 3 times, and detected with a donkey anti-goat IgG-FITC fluorescein(1:100, λ = 495 nm), in PBS containing 5% bovine serum albumin (BSA). Following another 3 PBS rinses, sections were counterstained with Hoescht 33258 (1:1000, λ = 395 nm:AnaSpec; San Jose, CA) to identify nuclei. Finally, the sections were then washed with PBS three times for 5 minutes each, before imaging.

IMAGING AND ANALYSIS

Hematoxylin and eosin sections were visualized with a Nikon Diaphot microscope mounted with an Optronix Microfire digital camera. Histological quantification of H&E was performed on each level and within each region of the ECM with the 20x objective lens. Immunofluorescence was visualized with a Leica DM LB2 fluorescence microscope, visualized under the 20x objective lens, and photographed with a Leica DFC340FX digital camera *(*Leica Microsystems; Wetzlar, Germany). Histological quantification and PECAM quantification were performed in each region of the ECM (n = 3). Myofiber cross-sectional area (CSA) and PECAM+ structures were measured and visualized utilizing ImageJ software. The number of PECAM-positive structures within each region of the ECM implant was counted to determine the number of blood vessels/mm^2. Implant area was determined by measuring the CSA of the

implanted region. A vessel was only counted if its lumen was greater than 20 μm in diameter.

STATISTICAL ANALYSIS

Data are represented as mean ± SEM. Statistical analysis was performed utilizing ANOVA for analysis of group samples. Comparisons between data sets were performed utilizing Tukey's post hoc tests where available. Significance is defined as $p < 0.05$.

RESULTS

MORPHOLOGICAL ANALYSIS

The average mass of the surgically removed tissue was 307 ± 3.7 mg wet weight, a value that accounts for approximately 27 % of the total mass of the LGAS. No significant differences in defect mass between groups were witnessed. The mass of the defect allowed for a sizeable area to which view myofiber regeneration. Consistent with previous work within our lab, the overall morphology of the LGAS was maintained in all groups following 56 day recovery post injury (Merritt et al., 2009). Restoration in the mass of the injured LGAS reached values of 81.2 ± 1.9% of the mass of the contralateral LGAS. However, no significant differences in injured LGAS mass recovery were seen between groups.

FUNCTIONAL ANALYSIS

Functional analysis at day 56 of recovery found maximal isometric tetanic force (P_O) produced in the saline group to measure 47.3 ± 4.2% of that produced in the contralateral LGAS, a value substantially lower than control. No significant differences were seen in P_O produced by the injured LGAS between the saline group and all other groups or in any other interactions (Figure 2). However, when P_O was observed between nerve (60.3 ± 4.4%) and non groups (48.9 ± 2.5%) compared to contralateral, a significant difference was observed between the two groups (Figure 3).

When maximal tetanic force was measured per unit of cross sectional area (CSA), known as Specific tension (SPo), a significant difference was seen in the Nerve+

PEG+MSC group (86.3 ± 5.8% of the contralateral LGAS) in comparison to Saline (62.9 ± 5.5%), PEG (54.6 ± 3.8%), and Nerve+PEG (57.1 ± 2.8%) groups ($p < 0.05$) (Figure 2). Interestingly, although not significant, PEG only and PEG+Nerve groups decreased both the maximal tetanic tension and the specific tension of these groups.

Additionally, mass of VML injury, Po, and SPo in non-nerve and nerve groups were compared to previous work done within our lab. A look at mass of tissue removed from the LGAS of the rat revealed significantly more tissue removed in this study compared to previous neurotization work done within this laboratory. A significant difference in mass between both non-nerve (305.3 ± 6.9 mg) and nerve groups (309.7 ± 3.6 mg) compared to non-nerve (189.5 ± 5.2 mg) and nerve (177.9 ±4.2 mg) in the previous study (Tierney et al., 2009, unpublished) (figure 4). Maximal tetanic tension in this study was significantly lower for nerve (75.1 ± 1.9%) and non-nerve groups (82.1 ± 4.3%) in comparison to Tierney et al., nerve (88.4 ± 2.6%) and non-nerve groups (92.9 ± 2.6%), (Figure 5). This decrease in function was also observed when tissue cross sectional area was accounted for, between nerve (82.1 ± 4.3%) and non-nerve groups (75.1 ± 1.9%) in comparison to nerve (94.9 ± 2.5%) and non-nerve groups (88.4 ± 2.6%) from Tierney et al., (Figure 6).

HISTOLOGY

Histological analysis of the defect area following 56 days of recovery demonstrated myofiber infiltration within the ECM. Cellular material staining by hematoxylin and eosin in the top, middle, and bottom regions of the ECM showed

cellular infiltration throughout all regions of the ECM. Myofiber cross sectional area was measured in the bottom (8a), middle (10a), and top (12a) of the implanted ECM. All regions contained small myofibers with nuclei centralized throughout the ECM. All groups in all regions of the ECM displayed left skewiness in cross sectional area of the myofibers; however, the phenotype for smaller, regenerating myofibers was slightly recovered in all regions by neurotization of the ECM. All groups showed dense packing of cellular content proximal to implantation borders where the ECM was sutured onto the tissue.

Hematoxylin and eoisn staining showed fibers in the bottom portion of the ECM that were both regenerating, in the process of maturing, or mature, as is evidenced by the location of nuclei either centrally or in the periphery of the cell (Figure 7). Visual analysis showed myofibers that were larger for all groups compared to the saline group (Figure 7). Measurement and quantification of myofibers of average size between 4000 μm^2 and 6500 μm^2, showed a significant difference in PEG, MSC, Nerve, and NervePEGMSC groups compared to Saline treatment (Figure 8B). Additionally, PEGMSC, NervePEG, and NervePEGMSC displayed significant difference in average size of the myofibers compared to both PEG and Nerve groups. Furthermore, there was a significant increase in average myofibers in both the MSC and NervePEG group in the bottom region of the ECM compared to the NervePEGMSC.

Visual analysis of H&E staining of the middle region of the ECM saw myofibers that were much smaller, less densely packed, and expressed central nucleiation (Figure 9). Further examination of CSA of averaged sized myofibers, between 4000- 6500 μm^2,

revealed significant differences in CSA in the middle region of the PEGMSC, Nerve, and NervePEGMSC groups in comparison to Saline (Figure 10B). Surprisingly, the Nerve group was the only group to display significant differences compared to PEG and NervePEG groups.

Examination of the top region of the ECM showed myofibers that were larger in size and morphologically similar to uninjured tissue but continued displaying regenerative patterns of central nucleiation, although less frequently in the NervePEGMSC group (Figure 11). Quantification of cross sectional area of average myofibers 4000-6500μm² revealed no significant differences between groups in this region of the ECM.

IMMUNOHISTOCHEMISTRY

Immunohistochemical analysis showed angiogenesis of the ECM in all regions. PECAM staining revealed blood vessel in all regions of the ECM, while the presence of central nuclei, identified by Hoechst 33258, substantiate the presence of these blood vessels amid regenerating myofibers in the middle region of ECM (Figure 13). Quantification of blood vessels larger than 20μm in the top region revealed a significant difference in blood vessel density (BV/mm²) in the NervePEGMSC, Nerve, and NervePEG group compared to Saline (Figure 14). Additionally, a significant difference was also observed in NervePEGMSC compared to PEG and PEGMSC groups. Surprisingly however, quantification of blood vessel density in the middle region of the ECM showed a significant difference only in the NervePEGMSC group in comparison to

Saline and PEG groups (Figure 15). Lastly, blood vessel density was shown to increase significantly in the NervePEGMSC group compared to Saline (Figure 16). These increases indicate that NervePEGMSC treatment has a direct role in increasing blood vessel density within all regions of the implanted ECM.

DISCUSSION

Traumatic injuries incurred during combat by military personnel and in motor vehicle accidents, by the civilian population are often suffered in the extremities. These types of injuries are characterized by substantial muscle mass loss, decreased tissue regeneration, and subsequent functional deficits. Associated mental distress ensues after limb salvage surgeries due to the cosmetic and functional deficits that accompany such traumatic injuries. These injuries have been associated with significant medical costs, consisting of initial hospital visits and subsequent therapies to regain function, as well as costs associated with disability compensation. It is estimated that almost 3 billion dollars are spent in treatment and disability benefits for those suffering from volumetric muscle loss associated injuries. Therefore, it is imperative that treatments which maximize regeneration of myofibers and functional improvements be developed, in order to minimize both the medical and disability costs and the emotional distress felt by patients.

A volumetric muscle loss injury and subsequent ECM implantation results in deficient self –repair and associated and sustained functional loss even after 56 days of recovery, in accordance with previous work in our laboratory (Merritt et al., 2010, Tierney et al., 2010, Merscham-Banda et al., 2012). This phenotype was rescued by the combination treatment of neurotization of the plantar nerve on the ECM and MSC delivery via a PEGylated Fibrin gel. The combination of treatment significantly improved myofiber cross sectional area and blood vessel density and specific tension in the implanted ECM. Improved myofiber infiltration was also witnessed in the PEGMSC group and all nerve groups, indicating that MSCs and nerves play a role in muscle repair.

However, increases in blood vessel density were only associated with nerve treatments, indicating a direct role of nerve on angiogenesis.

Although unable to fully regenerate tissue morphology and function, our ECM constructs had the capability of allowing cellular, myofiber, and blood vessel infiltration without any further treatments. The deficiencies in function and self repair are likely a consequence of incomplete penetration, by infiltrating myofibers. Studies have shown that ruptures in muscle in excess of 3mm greatly hinder the reparative capacity of myofibers as transected end are not able to travel long distances in order to fuse together (Terada et al., 2002). Increases in cellular content within the ECM primarily occurred in the bottom and top regions indicating possible myofiber in-growth following VML creation. The exact mechanism of regeneration, however, was not within the scope of this study. It is likely however that cellular content increases occurred due to the role of MSC in one of three mechanisms: de novo myofiber formation, fusion to existing infiltrating myofibers, or through a paracrine/autocrine signaling mechanism that recruits other cells and repair mechanisms. Research has shown that MSC exerts its effects via two different mechanisms: they first migrate from the bone marrow and incorporate into the satellite cell niche, under the basal lamina, in order to repopulate that stem cell population, followed by mobilization and engraftment following injury (LaBarge and Blau, 2002). Many other studies have shown incorporation into the satellite cell niche, possibly indicating that MSC indirectly contributes to muscle repair by satellite cell repopulation which then can become activated for muscle repair and nuclei donation to myofibers. Other research has shown that MSC engraftment occurs *in vivo* and that as many as 10%

of myofibers show MSC engraftment leading to dystrophin recovery in animal models of Duchenne muscular dystrophy (Gussoni et al., 1999, Nitahara-Kasahara, 2012). Although engraftment has been shown to occur, the values of engraftment have been minimal in comparison to the functional recovery seen following MSC treatment. These low occurrences of engraftment and increased functional recoveries have led to the belief that MSC must have an impact on recovery by other mechanisms (Prockop, 2003, 2009). It is likely that MSC act on the VML model through paracrine action to increase cellular content. Studies have shown that MSC can act to prevent cellular apoptosis and decrease fibrosis, events that increase left ventricular function following MSC treatment (Shabbir et al., 2009). The increases in functional recovery following MSC treatment are likely a role of growth factor release by MSC, among which, are VEGF, TSG-6, and IGF (Shabbir et al., 2009, Lee et al., 2009, Prockop, 2009). Certainly, paracrine action of chemokine release, by MSC, aided in the recruitment of progenitor cells, that likely contributed to the increases we witnessed in cellular content of the implant.

Mesenchymal stem cell secretion of VEGF has been attributed to neoangiogenesis subcutaneously and in the VML model of injury (Al-Khaldi et al., 2003, Tierney et al., 2009). The effects of MSCs angiogenesis is seen in a study looking at CD31+ vessels following exercise, an increase in CD 31+ vessel size and NG2 proteogylcan positive arterioles was seen within a week of injection (Huntsman et al., 2013). However, in our study we found that MSC worked in conjunction with nerve groups to significantly increase blood vessel density within our ECM construct. PEGMSC showed no significant increases in blood vessel density making it unlikely the cause of the increase in blood

vessel density. It is possible however, that MSC exerts its role in conjunction with nerve in order to amplify its VEGF response. Recently, it has been determined that VEGF is expressed in neurons and hypothesized that it may act on axonal outgrowth, as well as in the recruitment of undifferentiated neural progrenitors (reviewed in Autiero et al., 2005). Recently, research has looked at the effects of nerve growth factor (NGF) secreted by peripheral neurons on endothelial cells and it has been suggested that NGF acts on VEGF by stimulating its production. Research on the role of NGF on angiogenesis, found that NGF treatment alone or in concert with 6-hydroxy-dopamine (6-OHDA), a neurotoxic, elicited an up-regulation of VEGF in superior cervical ganglia and subsequent angiogenesis, an effect that was higher in combination than with NGF alone (Calza et al., 2001). In a similar study looking at the role of NGF on angiogenesis, following ischemia, found that NGF blocking impaired the angiogenic response in comparison to local NGF supplementation, which increased the rate of perfusion recovery (Emanueli et al., 2002). These studies indicate that neurotization of the construct alone can elicit a strong angiogenic response via secretion of NGF and its role on up-regulation of VEGF. This falls in accordance with our results that treatments involving nerve relocation significantly increase blood vessel density within the tissue construct and that pairing neurotization with a combined treatment, in this case MSC delivery would further increase blood vessel density. This combined effect is especially witnessed in the middle and top regions of the ECM construct, where the combined treatment significantly increased blood vessel density. In addition, satellite cells have been witnessed to reside in close proximity of blood vessels, a study in which blood capillary numbers were reduced

by 45%, saw a decrease in more than half the mean of satellite cells (Christov et al., 2007). This study indicates the complexity of involvement between the many factors that increase regeneration in the skeletal muscle. Additionally, other studies have shown that neuregulin-1 acts on the SC population by promoting differentiation (Hirata et al., 2007). It is possible that both MSC and nerve secrete growth factors that stimulate and enhance the secretion of VEGF to increase blood vessel density, while subsequently MSCs repopulate the SC which are affected by blood vessels, which then engraft onto the damaged tissue.

Despite morphological regeneration and blood vessel increases observed in the nerve groups and in the MSC groups. Functional improvements were only observed following 56 days of recovery in specific tension of the combined, NervePEGMSC group and Nerve only group. This characteristic is likely attributed to the significant increases seen in blood vessel density of the ECM, coupled with significant increases in cellular infiltration in the middle region of the ECM in these groups. While other groups showed increases in myofiber infiltration within the middle region of the ECM, it is possible that treatments have the ability to increase cellular infiltration via chemokine secretion but sustained function of these new myofibers occurs only in the presence of significant blood vessel density. Studies have highlighted the importance of vascularization and innervation of newly regenerating muscle fibers to the morphological and functional recovery of the injured muscle (Jarvinen, M., 1976a). The possibility that blood vessel number aid in regeneration via their role in gas, chemokine, and other biofactor exchange, in treatment groups that also displayed an increase in cellular content in the

middle region, is highlighted by our results showing a functional increase in Nerve and NervePEGMSC groups. These two treatments were the only two groups that displayed both increased cellular content in the middle region of the ECM and increased blood vessel density.

In summary, this study reveals that the treatment of a VML injury with MSCs in a PEGylated Fibrin hydrogel and plantar nerve implantation significantly improves histological, morphological, and functional recovery over ECM implantation alone. The combination of neurotization of the ECM construct seeded with MSC via PEGylated Fibrin gel significantly improves blood vessel density, a characteristic that either indirectly, through its associatetion with the nerve, or directly through gas and waste exchange with the tissue, improves function. The exact mechanism by which the combined treatment aids to restore function remains unclear and was not within the scope of this study, however it is hypothesized that it functional improvements occur via release of trophic factors by the ECM, nerve, and MSCs which recruit progenitor cells. Although function and histology of PEGylated groups did not significantly differ from Saline groups, future studies could observe the role of growth factor delivery on muscle regeneration in the VML model. Additionally, future studies could characterize macrophage phenotypes within the VML model in order to establish the role of macrophages in tissue remodeling and regeneration following treatments. Macrophage characterization and time course of infiltration would likely provide great insight to VML treatments, due to the role distinct macrophage populations play in hampering or increasing regeneration. Thus this work and future studies could play a beneficial role in

finding better clinical applications that would enhance tissue regeneration and function in military and civilian populations.

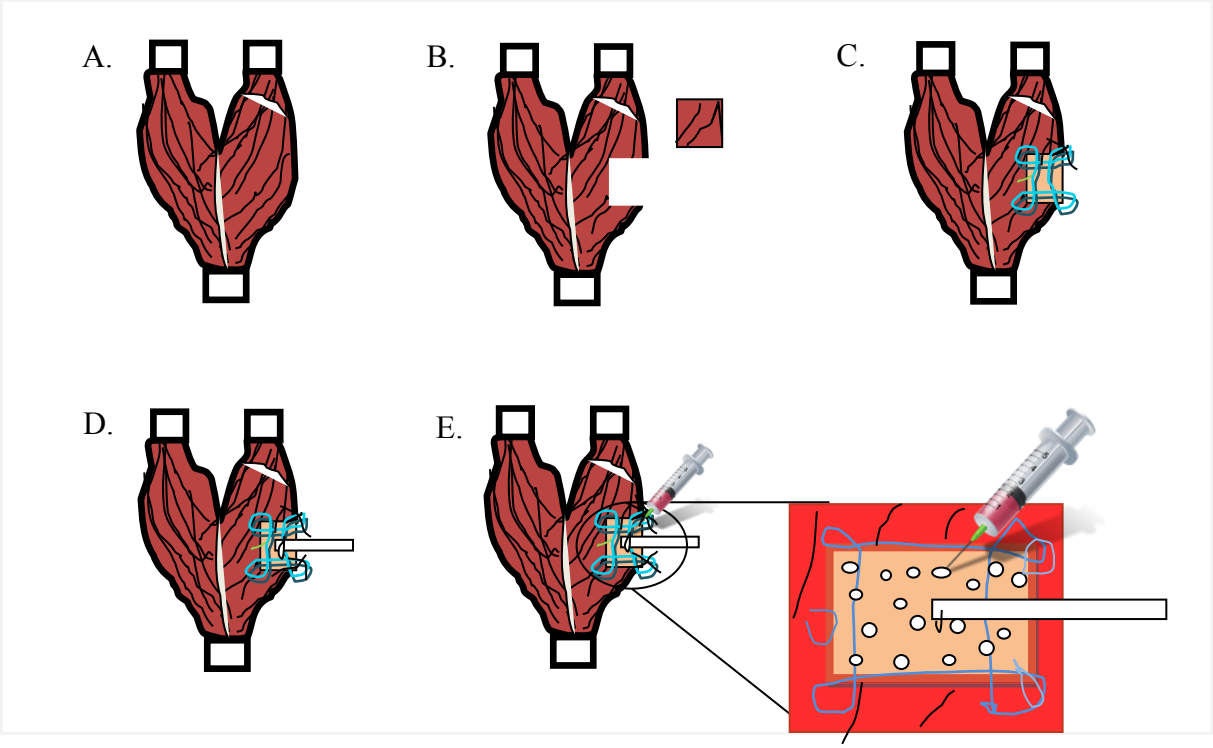

Figure 1: Schematic diagram of surgical procedures in VML injury model. A.) Uninjured LGAS. B.) Creation of 1x1cm VML injury. C.) Repair of injury with ECM using a modified Kessler stitch. D.) Neurotization procedure using Plantar nerve. E.) Injection of Saline, PEG, or PEG + MSC, 7 days post injury.

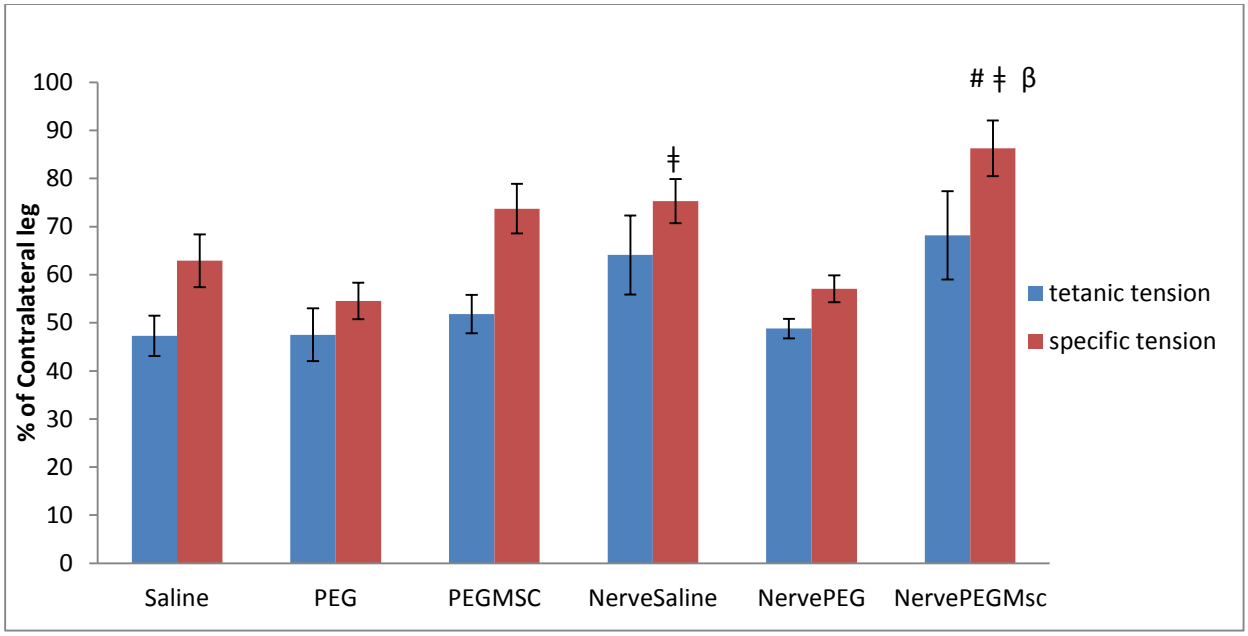

Figure 2: Functional recovery in LGAS. Tetanic tension (Po) and specific tension (SPo) following 56 days of recovery of the LGAS relative to the contralateral limb. ♯ indicates significance from SAL group. * indicates significance from PEG group. β indicates significance from NervePEG group. Significance is set at $p < 0.05$.

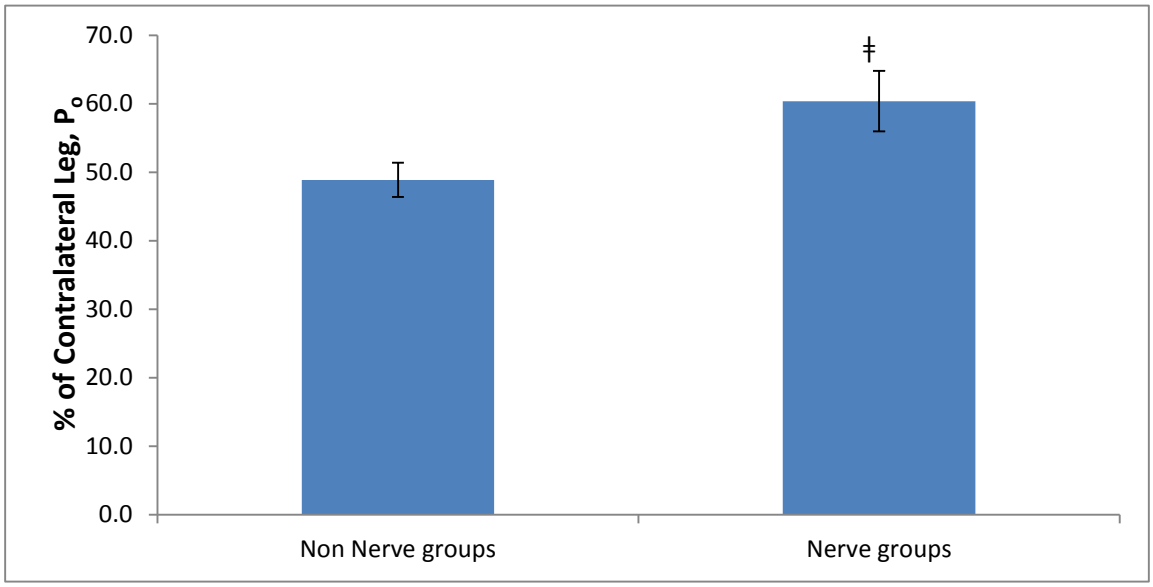

Figure 3: Tetanic Tension in LGAS. Tetanic tension (Po) following 56 days of recovery of the LGAS relative to the contralateral limb for Non Nerve and Nerve groups. ǂ indicates significance from Non Nerve group. Significance is set at $p < 0.05$.

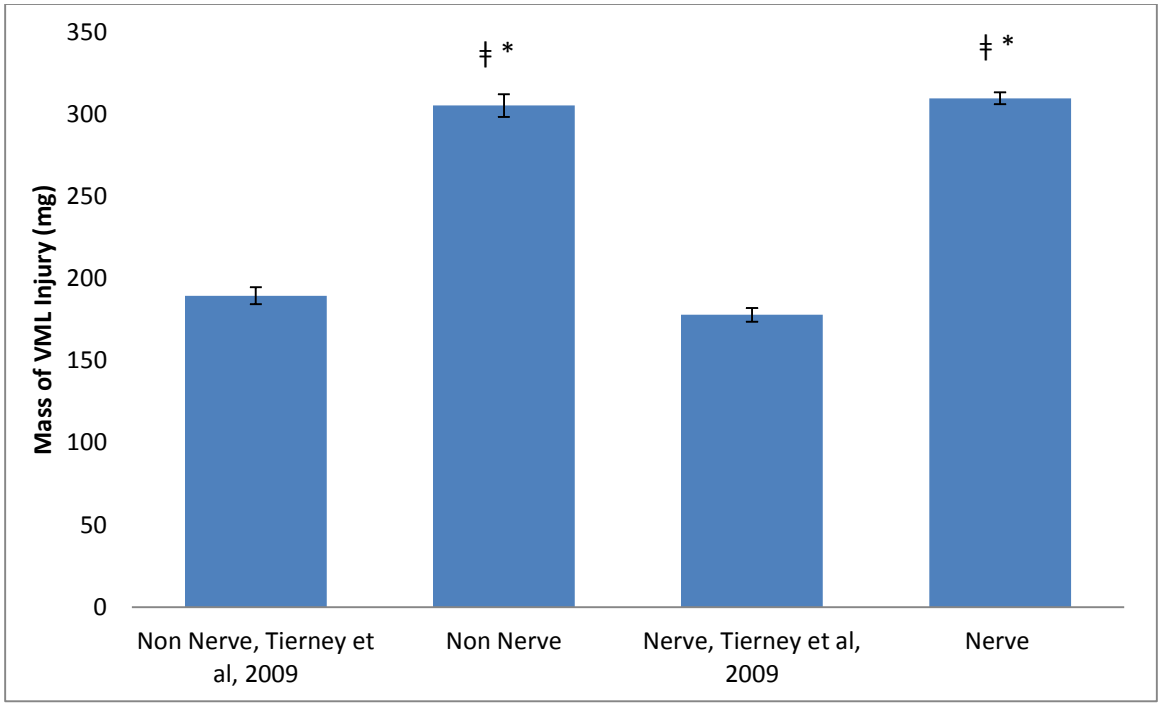

Figure 4: Mass of VML creation. Mass of injury created in LGAS of Tierney et al, 2009 and current study. ǂ indicates significance from Tierney et al, 2009 Non Nerve group. * indicates significance from Tierney et al, 2009 Nerve group. Significance is set at $p < 0.05$.

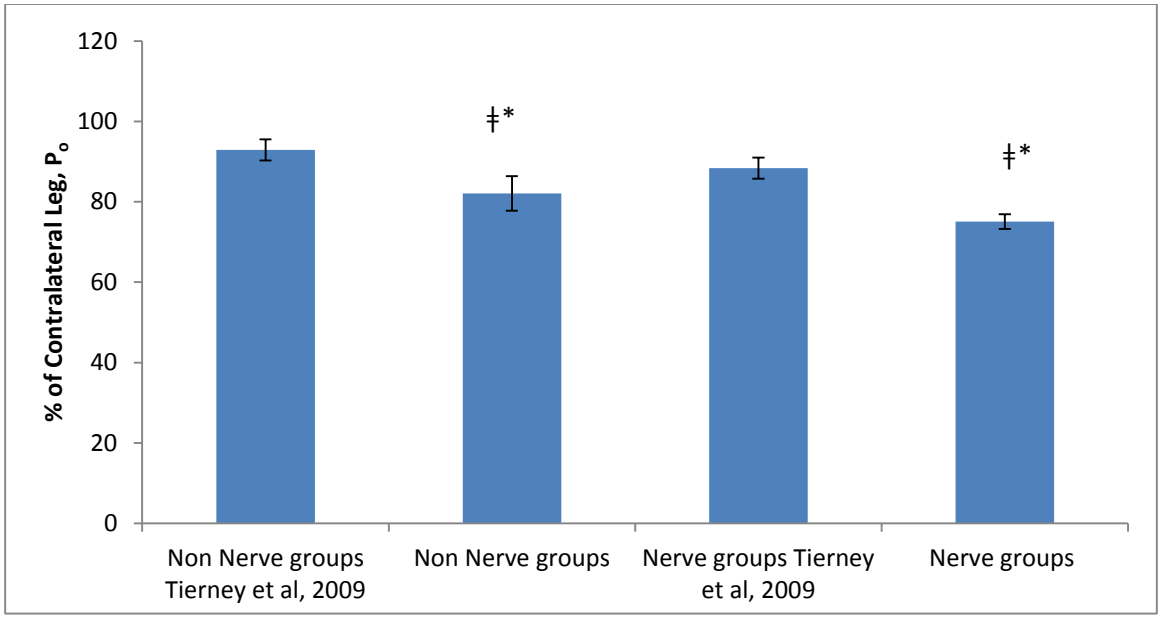

Figure 5: Tetanic Tension Comparison. Tetanic tension (Po) following recovery of the LGAS after 56 days, relative to the contralateral limb for Non Nerve and Nerve groups, within the current study and in Tierney et al, 2009. ǂ indicates significance from Tierney et al, 2009 Non Nerve group. * indicates significance from Tierney et al, 2009 Nerve group. Significance is set at $p < 0.05$.

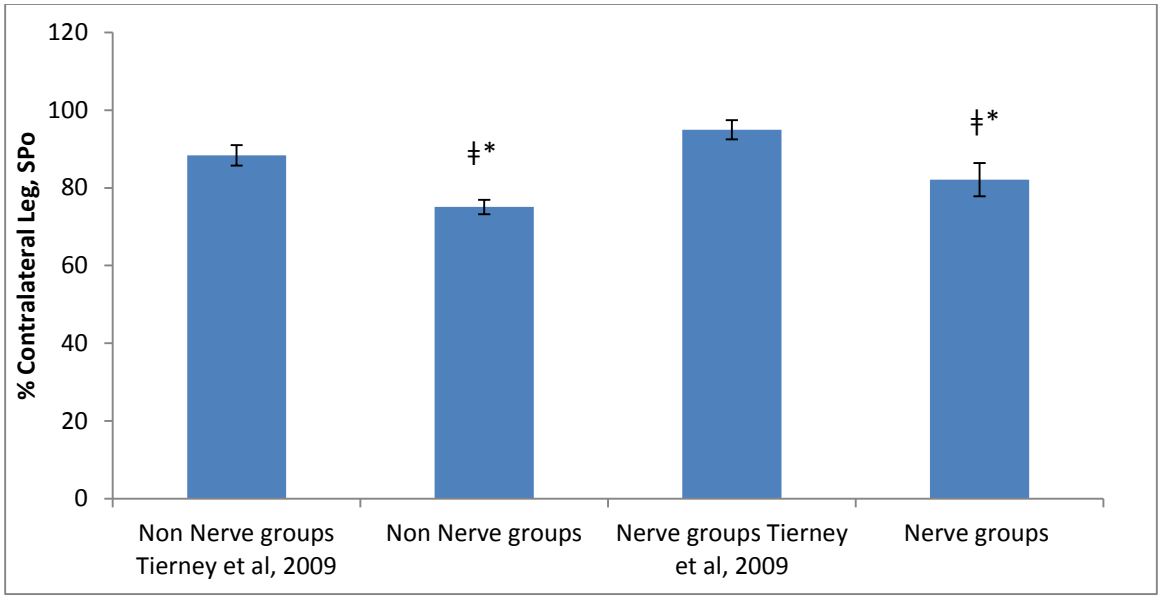

Figure 6: Specific Tension Comparison. Specific tension (SPo) following recovery of the LGAS relative to the contralateral limb for Non Nerve and Nerve groups in the current study compared to Tierney et al, 2009. ǂ indicates significance from Tierney et al, 2009 Non Nerve group. * indicates significance from Tierney et al, 2009 Nerve group. Significance is set at $p < 0.05$.

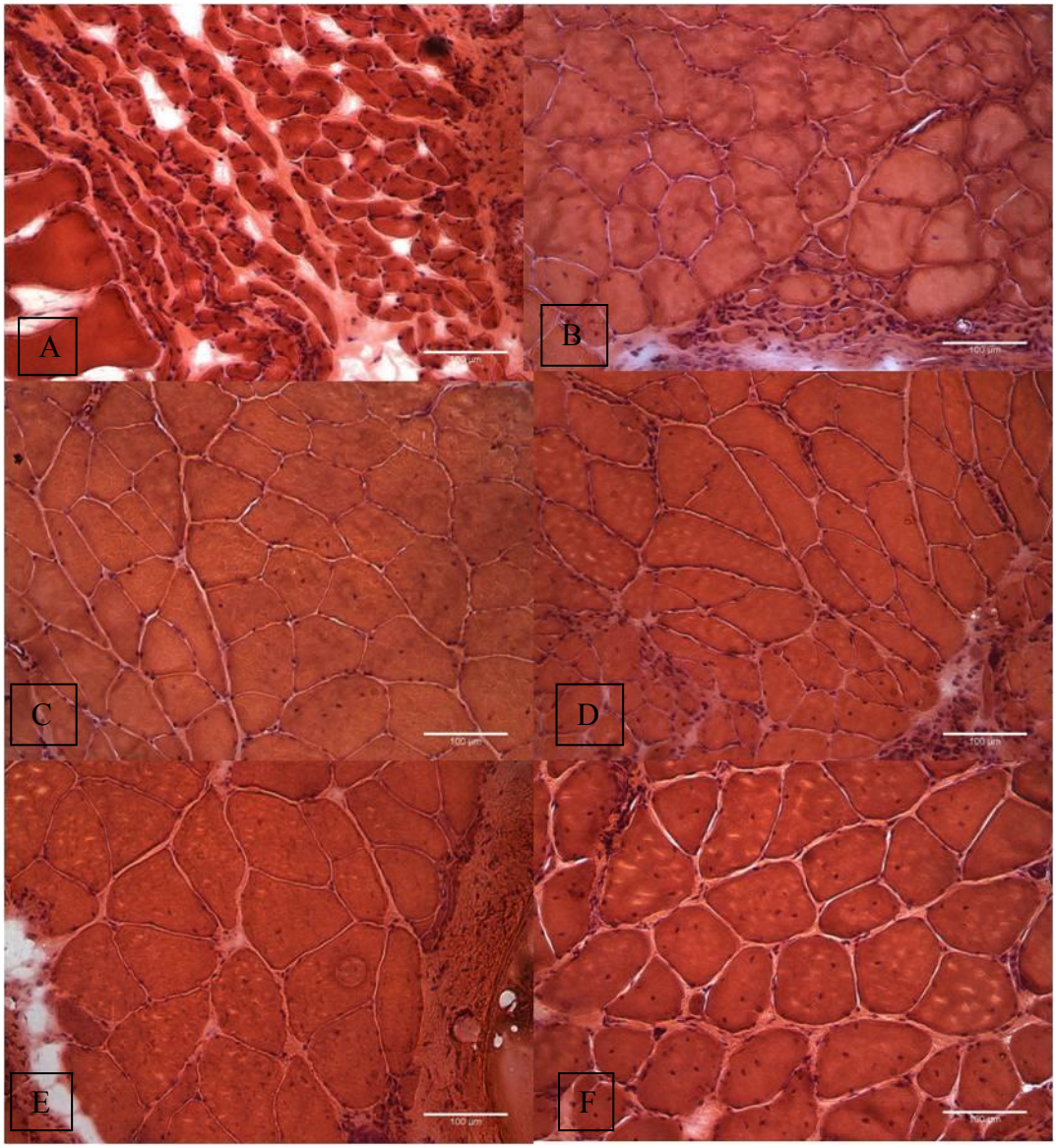

Figure 7: Hematoxylin and eosin staining. Myofiber infiltration with H& E staining in bottom region of ECM implant taken with 20x objective lens. (A.) SAL group (B.) PEG group (C.) PEGMSC group (D.) NERVE group (E.) NERVEMSC group (F.) NERVEPEGMSC group Scale bar = 100 μm.

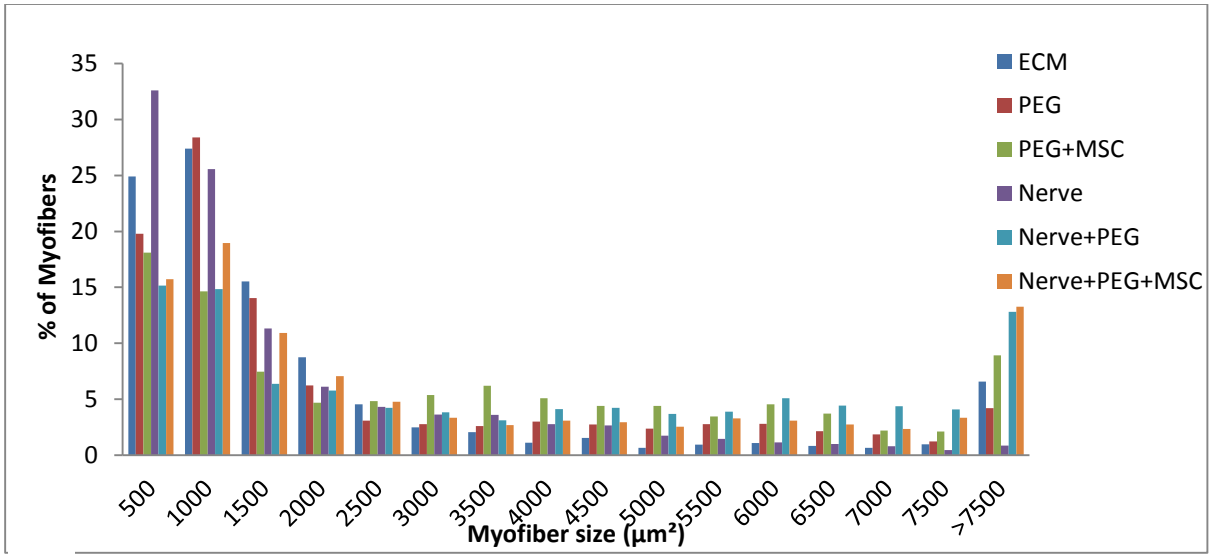

A

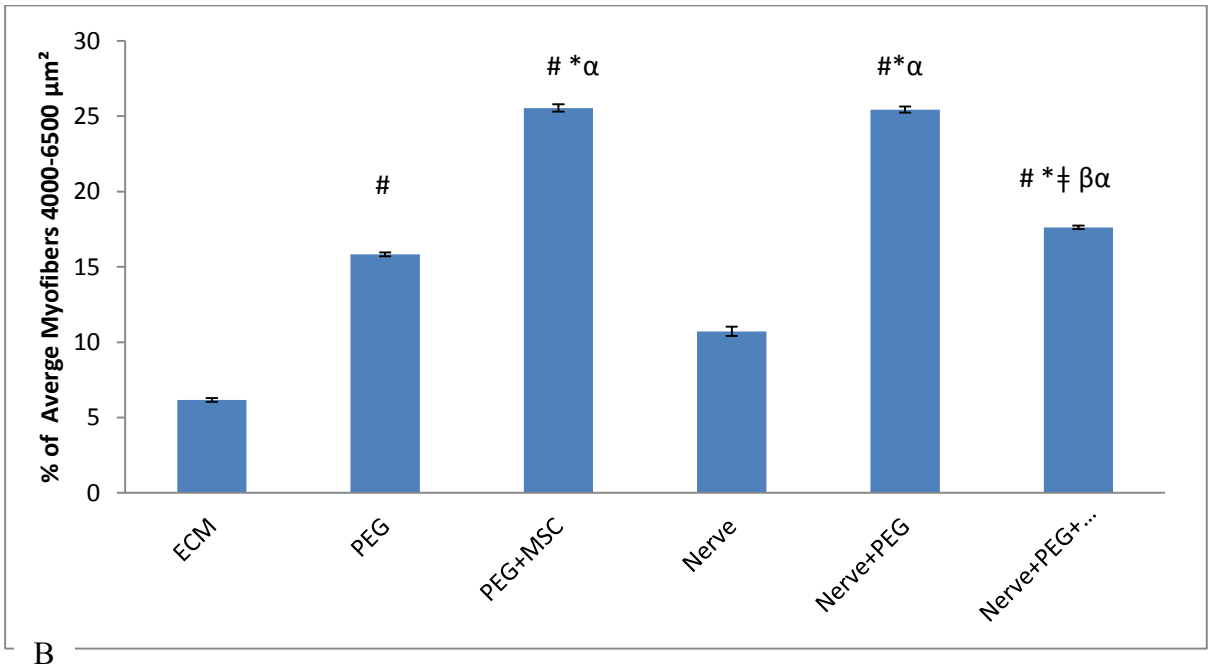

B

Figure 8: Cross sectional area of bottom region of VML. CSA was determined through Hematoxylin & Eosin staining. A.) Fiber size distribution was determined in the bottom region of the ECM. B.) Proportion of average fibers between 4000 µm² and 6500 µm² compared to total fibers. # denotes significant difference compared to ECM. * Denotes significant difference compared to PEG only. ǂ denotes significance compared to MSC group. α denotes significance compared to Nerve only. β denotes significance compared to Nerve+ PEG. Significance is set at $p < 0.05$.

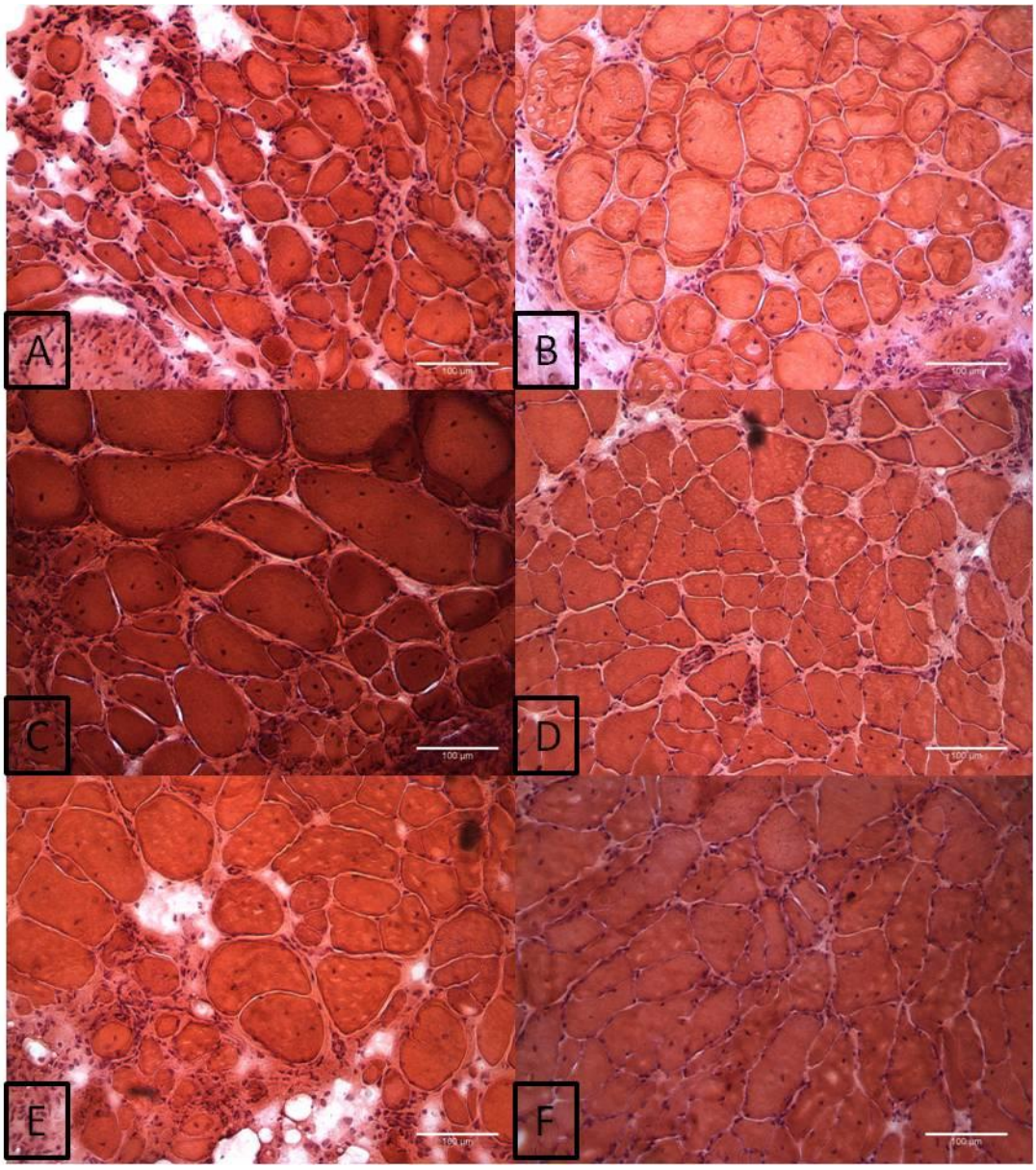

Figure 9: Hematoxylin and eosin staining. Myofiber infiltration with H& E staining in middle region of ECM implant taken with 20x objective lens. (A.) SAL group (B.) PEG group (C.) PEGMSC group (D.) NERVE group (E.) NERVEMSC group (F.) NERVEPEGMSC group Scale bar = 100 μm.

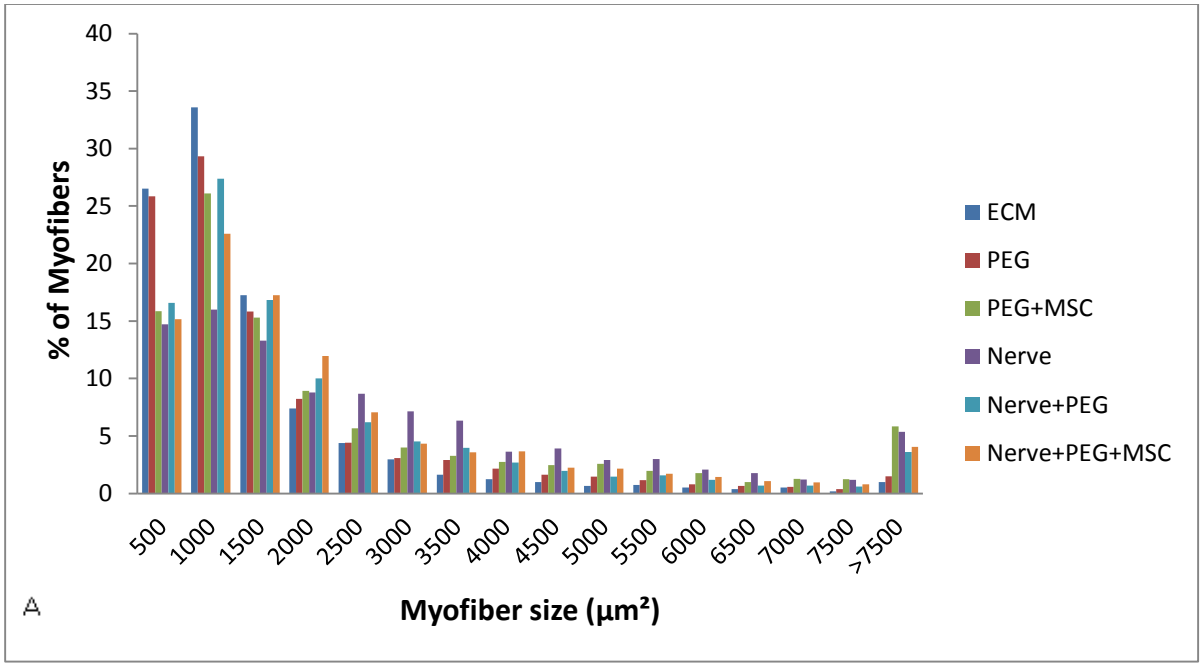

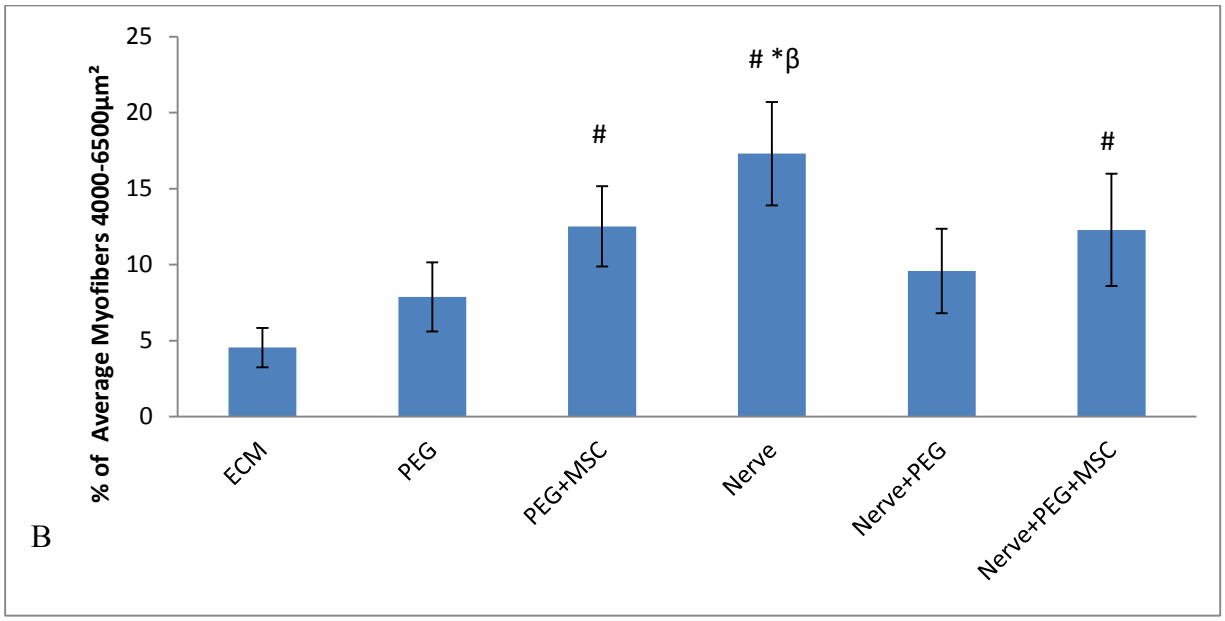

Figure 10: Cross sectional area of middle region of VML. CSA was determined through Hematoxylin & Eosin staining. A.) Fiber size distribution was determined in the middle region of the ECM. B.) Proportion of average fibers between 4000 µm² and 6500 µm² compared to total fibers. Muscle fiber CSA was compared among all treatment groups. # denotes significant difference compared to ECM. * Denotes significant difference compared to PEG. β denotes significance compared to Nerve+ PEG. Significance is set at $p < 0.05$.

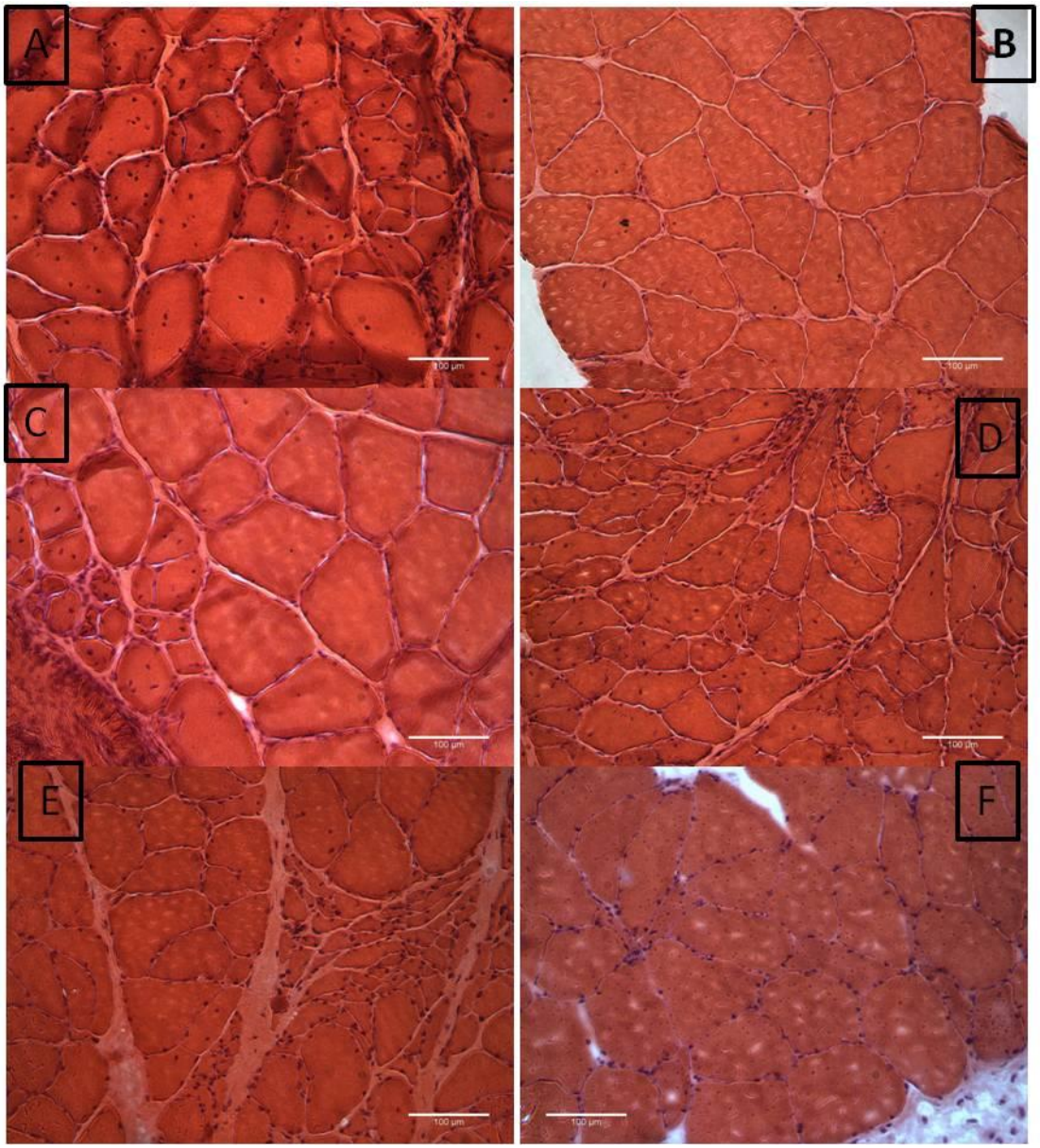

Figure 11: Hematoxylin and eosin staining. Myofiber infiltration with H& E staining in top portion of ECM implant taken with 20x objective lens. (A.) SAL group (B.) PEG group (C.) PEGMSC group (D.) NERVE group (E.) NERVEMSC group (F.) NERVEPEGMSC group Scale bar = 100 μm.

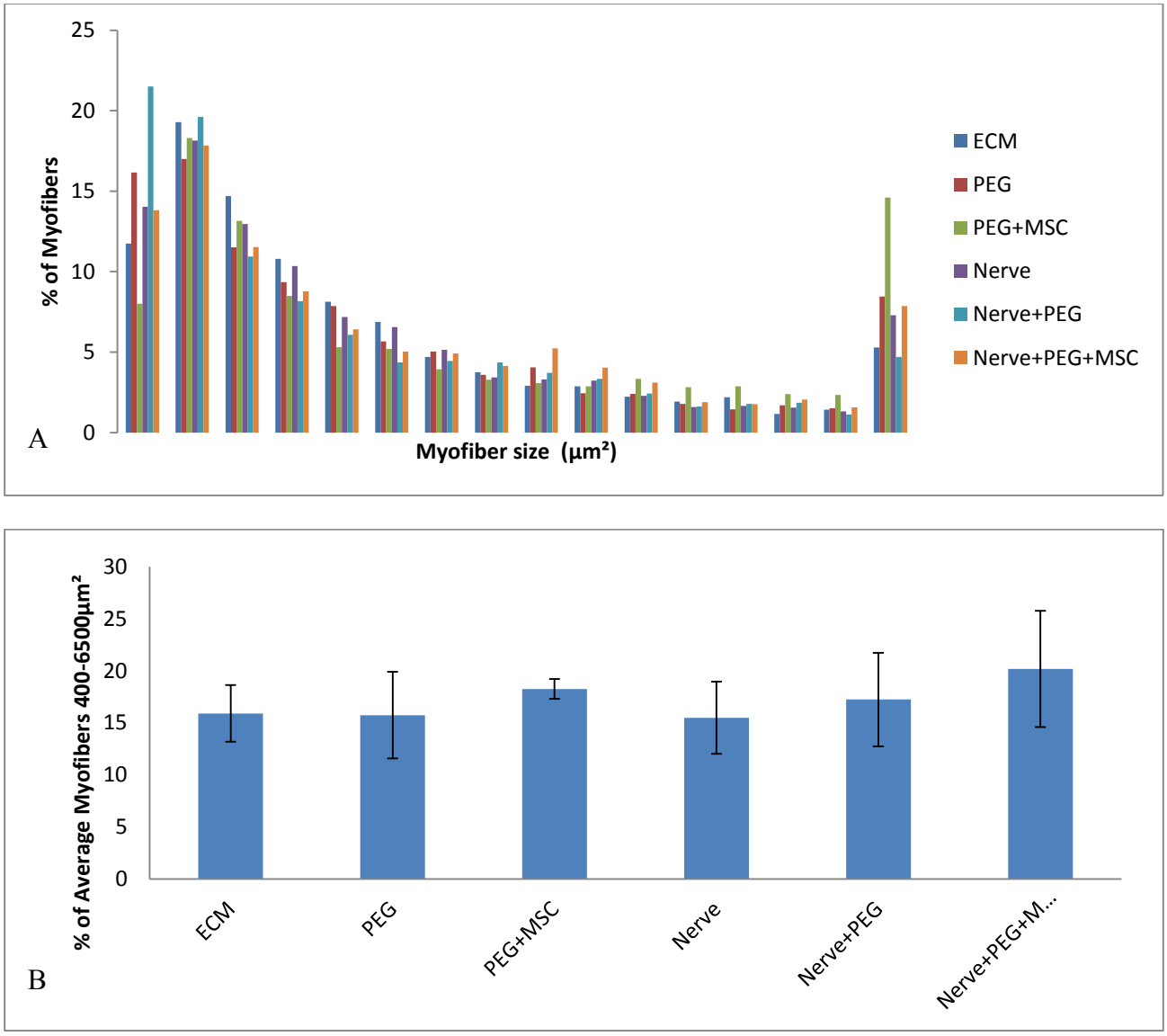

Figure 12: Cross sectional area of Top region of VML. CSA was determined through Hematoxylin & Eosin staining. A.) Fiber size distribution was determined in the top region of the ECM. B.) Percentage of average fibers between 4000 µm² and 6500 µm² compared to total fibers. Muscle fiber CSA was compared among all treatment groups. Significance is set at $p < 0.05$.

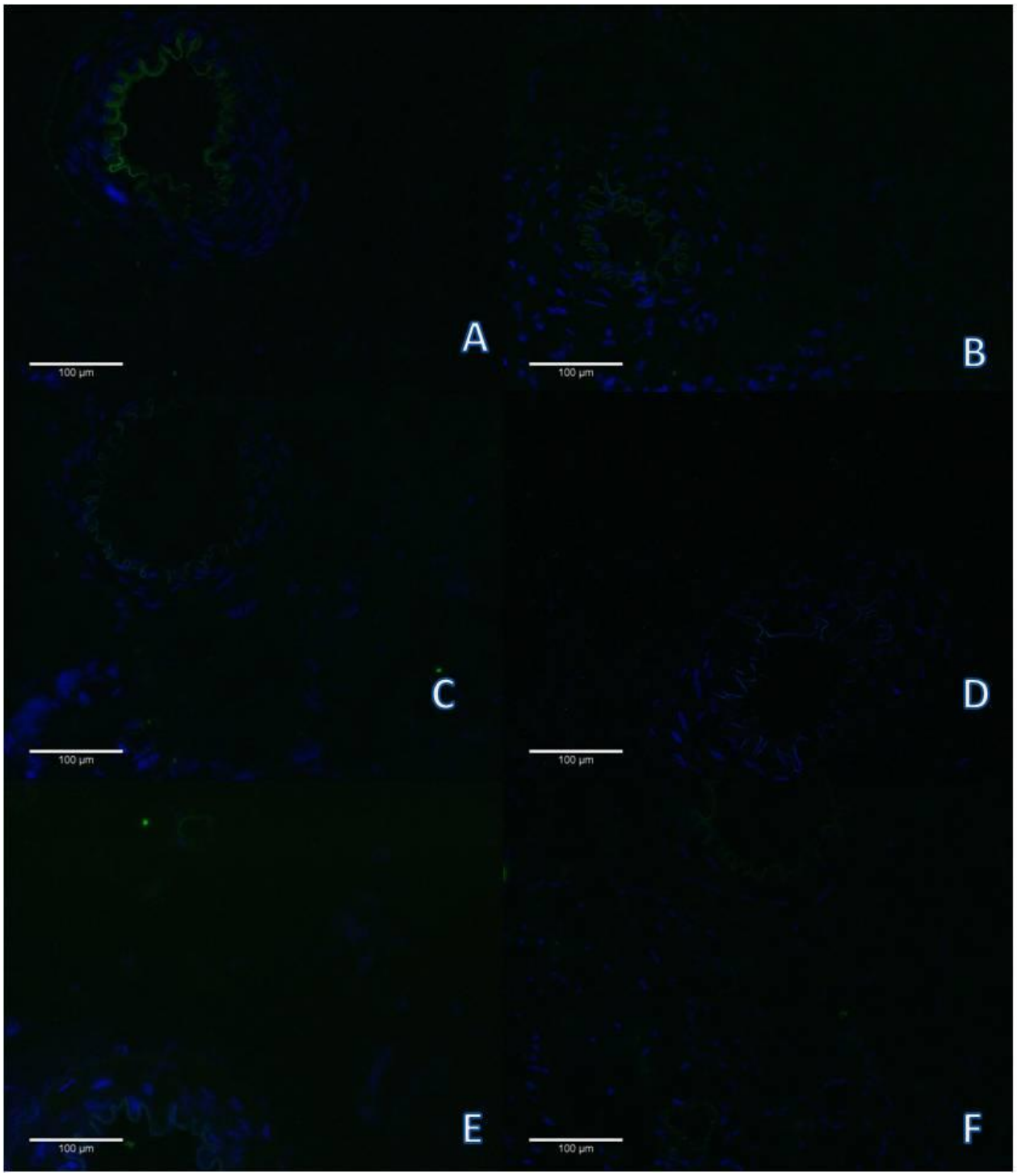

Figure 13: PECAM staining. Angionesis observed via PECAM staining in mid portion of ECM implant, image taken with 20x objective lens. Images taken of blood vessels ≥ 20µm. (A.) SAL group (B.) PEG group (C.) PEGMSC group (D.) NERVE group (E.) NERVEMSC group (F.) NERVEPEGMSC group Scale bar = 100 µm.

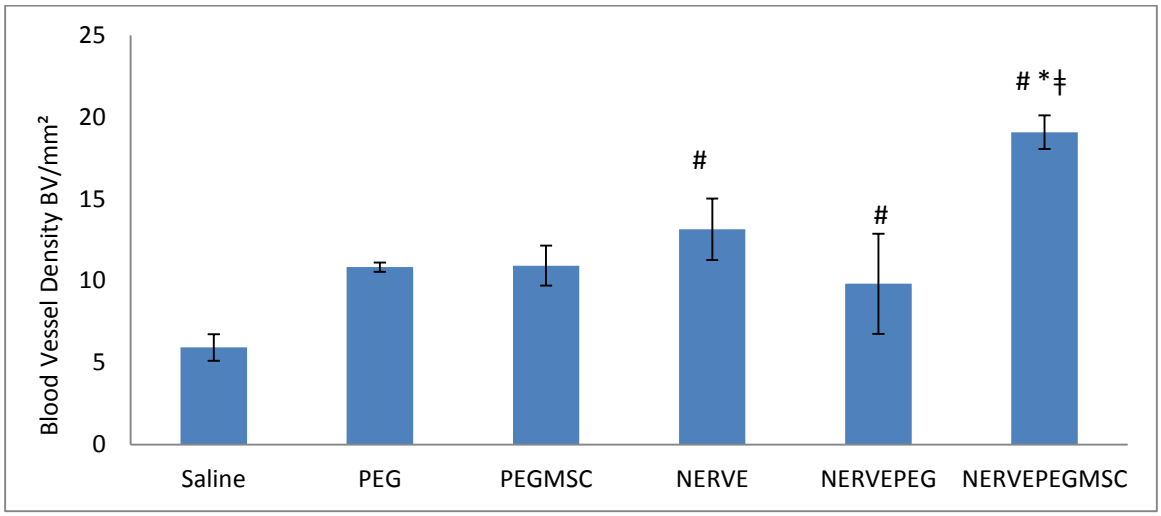

Figure 14: Blood Vessel Density in Top region of VML. Blood vessel density was determined through PECAM staining. Only blood vessels ≥ 20μm were counted. # denotes significant difference compared to ECM. * Denotes significant difference compared to PEG only group. ǂ denotes significance compared to MSC group. Significance is set at $p < 0.05$.

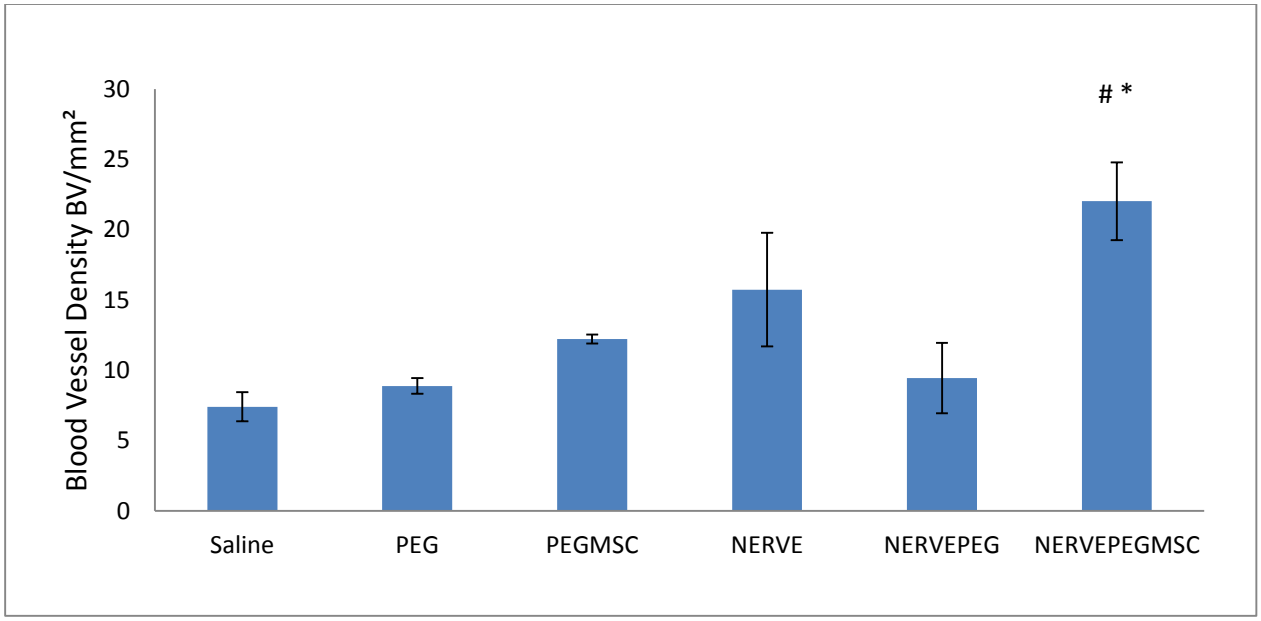

Figure 15: Blood Vessel Density in Middle region of VML. Blood vessel density was determined through PECAM staining. Only blood vessels ≥ 20μm were counted. # denotes significant difference compared to ECM. * Denotes significant difference compared to PEG only group. Significance is set at $p < 0.05$.

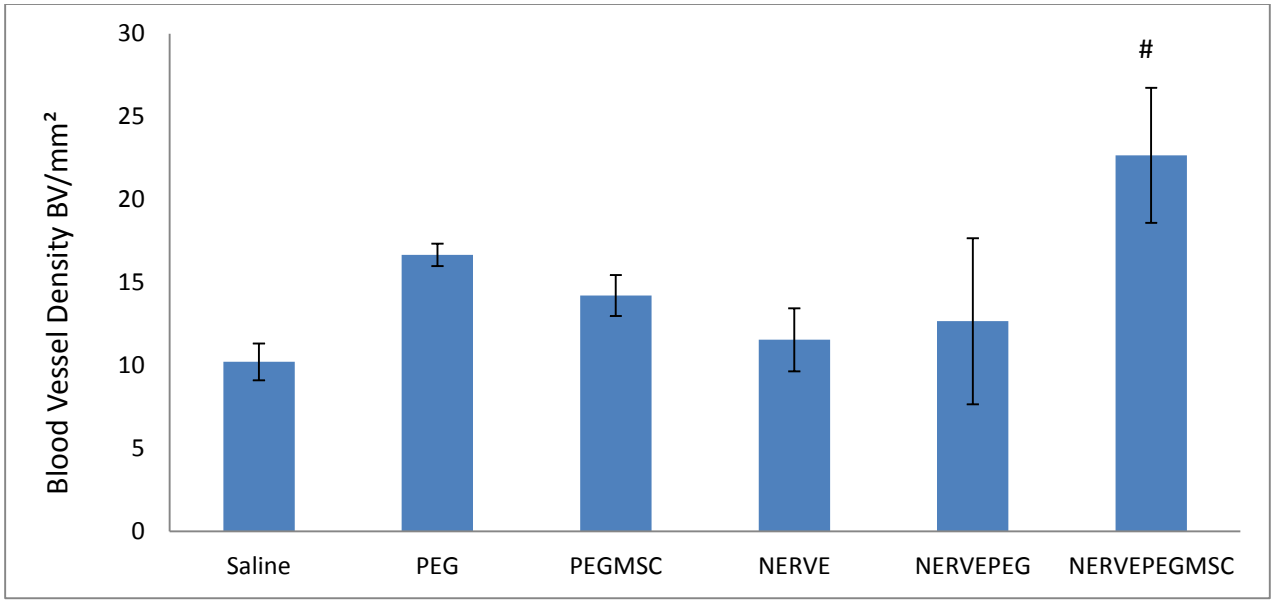

Figure 16: Blood Vessel Density in Bottom region of VML. Blood vessel density was determined through PECAM staining. Only blood vessels ≥ 20μm were counted. # denotes significant difference compared to ECM. Significance is set at $p < 0.05$.

APPENDIX A: EXPANDED METHODS

I. EXTRACELLULAR MATRIX DECELLULARIZATION:

1. Place separated gastrocnemius muscles in a 50ml conical tube with deionized (DI) water at 4°C for 24 hours.

2. Place muscle in electrophoresis tank

3. Fill electrophoresis tank with Tris-Glycine solution

4. Run electrophoresis machine at 15V for 6 hours.

5. Remove tissue after 6 hours running and place in SDS overnight

6. Repeat steps 2-6, until ECM is completely decellularized.

7. Rinse ECM in DI water for 72 hours.

8. Place the ECM in 70% ethanol for 4 hours.

9. Remove ethanol and place ECM in sterile PBS with 1% AA and expose to ultraviolet (UV) light for a minimum of 12 hours.

10. Store in PBS with 1%AA at 4°C until ready for implantation.

11. ECM not immediately decellularized are placed in glycerol solution for 24 hrs at 4°C.

12. Then transferred to the freezer until ready for decellularization.

II. VOLUMETRIC MUSCLE LOSS & REPAIR

1. Autoclave all instruments that will come into contact with the animal, including bench liners. Observations should be made every 15 minutes for the duration of the surgical procedure.

2. Weigh and anesthetize the animal until absence of withdraw reflex is seen.

3. Give analgesic, .01ml/g

4. Shave the hindlimb in which the defect will be created.

5. Using a scalpel cut a two-centimeter incision on the lateral side of the lower leg, parallel with the tibia.

6. Separate the biceps femoris from the tibia to expose the LGAS.

7. Separate the soleus from the LGAS and place a small aluminum foil plate between the soleus and LGAS to prevent injury to the soleus upon defect creation.

8. Using two scalpel blades separated by a 1cm spacer, create the full-thickness defect distal to the neuromuscular junction and in line with the tibial tuberosity.

9. Cut the medial edge of the defect using a pair of fine surgical scissors, and weigh the excised tissue.

10. Cut a piece of the extracellular matrix roughly the same dimensions as the tissue excised and implant it into the area of defect.

11. Using a modified Kessler stitch, suture the ECM with non-absorbable 5-0 polyprolene sutures.

12. Stitch simple sutures at the proximal, distal, and medial portions of the ECM to mark the edges of the ECM for later analyses.

13. Close the wound by suturing the biceps femoris utilizing simple interrupted stitches. Suture the skin incision using simple interrupted sutures with the knot tied underneath the skin to ensure the animal does not open the wound.

14. Return animal to cage and monitor until animal has regained consciousness and mobility.

15. Monitor animal for the next 48 hrs.

16. Give subcutaneous analgesic .01ml/g at 12 hrs, 24, and 48 post surgery.

III. A. BONE MARROW DERIVED MESENCHYMAL STEM CELL ISOLATION:

1. Prior to bone marrow isolation, sterilize all instruments and warm two 50 ml conical tubes containing media to 37°C in the water bath.

2. Fill two sterile petri dishes with sterile DPBS.

3. Anesthetize the animal and shave the hindlimbs.

4. Surgically remove both femurs and tibias. Remove as much muscle and connective tissue as possible, and place bones in one of the DPBS filled petri dishes.

5. Allow bones to sit in DPBS for a few minutes. This will help in further removal of any remaining tissue on the bones.

6. After cleaning the bones a second time, cut the epiphyses of the bones and place in second DPBS filled petri dish. Transport dish to the tissue culture hood.

7. Place one of the media tubes from the water bath under the hood.

8. Obtain four sterile 50 ml conical tubes (one for each bone) and place under the hood.

9. Using an 18-G needle attached to a 3ml syringe, draw up some media and flush out the bone marrow of each bone. Use a total of 10 ml of media per bone, for each tube.

10. Mechanically disrupt bone marrow clumps by drawing the bone marrow containing media up and down using a series of smaller syringes (16G, 18G, 21G).

11. Transfer media in each of the 50 ml tubes to 15 ml conical tubes (one for each bone).

12. Centrifuge the tube at 1000 x g for 5 minutes at 4°C.

13. Remove the supernatant and resuspend the pellet in 3 ml of media.

14. Obtain four 25 cm2 tissue culture flasks and plate the cells (one tube per flask). Add 7 ml of media to each flask, for a total of 10 ml of media per flask.

15. Place flasks in incubator set at 37°C and 5% CO2 for 24 hours.

16. Remove media (this is the non-adherent fraction) from flasks and place in four sterile 15 ml conical tubes. Centrifuge and plate as described above.

17. Rinse the first set of flasks at least twice with DPBS to remove remaining RBCs and debris.

18. Change media and rinse the flasks with DPBS for the next two consecutive days.

19. After this time period, change the media every 2-3 days until the cells have reached ~80% confluency and the cells must be split.

IV. MSC CULTURE:

Media Preparation:

1. Control media is made up of 90% Dulbecco's Modified Eagles Medium (DMEM) + 10% Fetal Bovine Serum (FBS) + 1% Antibiotic/Antimycotic (AA)

2. In a sterile 50 ml conical tube, add 45 ml of DMEM + 5 ml FBS + 1 ml AA.

3. Store media at 2-8°C.

4. Prior to use, warm media in 37°C water bath for at least 15 minutes.

Changing Media:

1. Cells should be monitored microscopically daily, and confluency should be noted.

2. Media should be changed every 2-4 days.

3. To change media, aspirate old media, rinse flask twice with DPBS and replace with 10 ml of fresh media.

4. When cells have reached ~80% confluency, they must be trysinized.

Passaging Cells:

1. Once cells have reached ~80% confluency, remove media from flasks and rinse twice with DPBS.

2. Replace DPBS with 3 ml 0.25% Trypsin/EDTA and place in incubator for three minutes.

3. Remove flasks from incubator and tap flasks against the side of a table to induce detachment of cells. Use the microscope to verify cells are detached.

4. Remove cell suspension from flasks and place in sterile 15 ml conical tube (one tube per flask).

5. Rinse flask with DPBS to obtain remaining cells, and place DPBS in appropriate tube.

6. Centrifuge tubes at 1000 x g for five minutes at 4°C.

7. Remove supernatant from tubes and resuspend in 3 ml of fresh media.

8. Split each tube into desired number of flasks. Prior to adding cell suspension to flasks, place 7 ml of media into each flask, for a total of 10 ml of media per flask.

9. Place flasks in incubator at 37˚C and 5% CO_2.

Cryopreservation:

1. In the event that cells must be frozen for future use instead of passaged, carry out steps 1-6 as described in the previous section.

2. After centrifugation, resuspend cells in 1ml of freezing medium.

3. Place cell suspension in a 2 ml cryotube and place in -80°C freezer for two days, after which, tube can be transferred to liquid nitrogen.

Thawing:

1. Obtain cells from liquid nitrogen storage and place 2 ml cryotube in 37°C water bath until a small amount of ice remains.

2. Place the 1 ml suspension in a sterile 15 ml conical tube, rinse cryotube with 1 ml DPBS, and place DPBS in conical tube.

3. Slowly pipette 4 ml of freshly warmed media into the conical tube, and gently pipette media up and down.

4. Centrifuge at 1000 x g for 5 minutes at 4°C.

5. Remove supernatant from tubes and resuspend in 3 ml of fresh media.

6. Split each tube into desired number of flasks. Prior to adding cell suspension to flasks, place 7 ml of media into each flask, for a total of 10 ml of media per flask.

7. Place flasks in incubator set at 37°C and 5% CO2.

V. IN SITU FUNCTIONAL ANALYSIS

1. Weigh and anesthetize the animal, and shave hindlimbs of both legs.

2. Create a 2 cm skin incision parallel to the femur to expose the biceps femoris.

3. Locate the origin of the biceps femoris and separate the connective tissue with forceps until they go through the biceps femoris.

4. Separate the tissue using hemostats until you can locate the sciatic nerve.

5. Cut the biceps femoris along the femur towards the hip.

6. Isolate the sciatic nerve from surrounding musculature and cut the nerve as close to the hip as possible.

7. Remove any remaining tissue from the sciatic nerve and tuck it back into place.

8. Make an incision along the midline of posterior portion of the lower limb from the calcaneus to the popliteal region.

9. Separate the skin from the biceps femoris, and cut the biceps femoris similarly to the skin to expose the LGAS.

10. Isolate the gastrocnemius from the biceps femoris.

11. Dennervate the MGAS. This will ensure force will be measured only in the LGAS.

12. Cut the calcaneus so that the distal portion of the gastrocnemius and Achilles tendon are still attached.

13. Separate the soleus and plantaris from the GAS by cutting the distal insertions.

14. Using the calcaneus to hold it in place, tie the Achilles tendon to the muscle lever arm of the dual-mode servometer.

15. To stimulate the LGAS, place electrodes connected to a muscle stimulator (Model 2100) on the sciatic nerve.

16. Keep the muscle warm with a radiant heat lamp, and occasionally moisten the muscle and nerve with mineral oil.

17. Using a micrometer, find the muscle's optimal length.

18. Stimulate the LGAS at 150Hz to determine peak tetanic tension. Allow two minutes of rest between contractions.

19. After functional analysis is completed, remove the gastrocnemius and other tissues of interest.

20. Carefully separate the MGAS and LGAS.

21. Weigh muscles and measure the length of the LGAS.

22. Freeze muscles in liquid nitrogen cooled isopentane and store in -80°C freezer.

VI. HEMATOXYLIN & EOSIN STAINING:

Hematoxylin & Eosin staining is one of the most used stains in histology to examine tissue morphology. Hematoxylin stains nucleic acids a deep blue-purplish color. Eosin stains cytoplasm, red blood cells and skeletal muscle fiber pink.

1. Using the tall Coplin jars, immerse slides in Harris Hematoxylin for five minutes.

*Pour out the solution and gently rinse in tap water until water runs clear.

2. Immerse slides in Eosin for two minutes.

* Pour out the solution and gently rinse in tap water until water runs clear.

3. Immerse slides in 70% ethanol for several seconds. Ethanol will dehydrate the section and remove excess eosin.

4. Pour out ethanol and immerse slides in 100% ethanol for several seconds.

5. Under the fume hood, immerse slides in Xylene for several seconds. Xylene will make the tissue hydrophobic so a coverslip can be applied with a resin in solvent (Permount).

6. Remove the slides from Xylene and allow slides to dry for 30 minutes in the hood.

7. Apply a coverslip using a few drops of Permount.

VII. PECAM AND HOECHST 33258 STAINING:

Immunofluorescence allows the visualization of specific proteins, through the binding of an antibody to the protein of interest; a secondary antibody is then applied that is

chemically conjugated to a fluorescent dye. Under specific filters the protein of interest can be visualized.

1. Immerse slides in cold Acetone for 10 minutes.

2. Immediately, rinse slides with PBS 3 times for 5 minutes.

3. Place slides in humid box. Using a barrier pen, draw circles around specimen in order to prevent solutions from running of the slide.

4. Immerse slides in 10% normal serum in PBS for 20 minutes.

5. Rinse slides with PBS 3 times for 5 minutes.

6. Incubate tissue slides in PECAM-1, primary antibody (2:100), in the 4˚C refrigerator for 1 hour.

7. Rinse slides with PBS 3 times for 5 minutes.

8. Incubate tissue in 2˚ anti-body, (anti-goat conjugated to fitc) at room temperature for 45 minutes. (1:100)

9. Rinse with PBS 3 times for 5 minutes.

10. Incubate sections with Hoechst 33258 (1:1000) for 15 min.

11. Rinse with PBS 3 times for 5 minutes.

12. Image immediately following PBS washes.

APPENDIX B: RAW DATA

MASS AND FORCEMEASUREMENT DATA

Saline group														
				Defect (Left) Leg										
Animal	Group	Mass: Surgery (g)	Mass: FM (g)	Defect Mass (mg)	Def LGAS Mass (mg)	Def MGAS Mass (mg)	Def SOL Mass (mg)	Def PLAN Mass (mg)	Def LGAS Length (mm)	Def LGAS CSA (cm^2)	Def Tetanic Force (N)	Optimal Length (N)	Def Max Force (N)	Def Specific Tension (N/cm^2)
101	Saline ECM	451	494	264	760	-	-	-	29	0.65	9.15	0.55	9.70	15.02
105	Saline ECM	700	720	357	972	1247	235	486	32	0.75	5.80	0.60	6.40	8.55
103	Saline ECM	454	473	261	929	-	-	-	31	0.74	9.55	0.55	10.10	13.68
104	Saline ECM	512	543	293	888	1162	300	603	31	0.71	10.00	0.55	10.55	14.95
106	Saline ECM	601	636	287	892	1395	399	695	30	0.73	10.65	0.55	11.10	15.15
Mean:		**543.6**	**573.2**	**292.4**	**888.2**	**1268.0**	**311.3**	**594.7**	**30.6**	**0.7**	**9.0**	**0.6**	**9.6**	**13.5**
SEM:		**47.6**	**46.2**	**17.3**	**35.5**	**68.1**	**47.7**	**60.5**	**0.5**	**0.0**	**0.8**	**0.0**	**0.8**	**1.3**

Saline group													
	Contralateral/Control (Right) Leg												
Animal	Con LGAS Mass (mg)	Con MGAS Mass (mg)	Con SOL Mass (mg)	Con PLAN Mass (mg)	Con LGAS Length (mm)	Con LGAS CSA (cm^2)	Def Tetanic Force (N)	Optimal Length (N)	Def Max Force (N)	Con Specific Tension (N/cm^2)	LGAS Mass (% Contralateral)	Def Force (% Contralateral)	Specific Tension (% Contralateral)
101	1165	-	-	-	30	0.96	19.60	0.60	20.20	21.11	65.2	46.7	71.2
105	1205	1154	266	393	33	0.90	18.00	0.60	18.60	20.67	80.7	32.2	41.4
103	1170	-	-	-	32	0.90	17.25	0.55	17.80	19.76	79.4	55.4	69.2
104	1094	1089	302	456	32	0.84	18.30	0.60	18.90	22.44	81.2	54.6	66.6
106	1300	1283	328	497	32	1.00	22.30	0.60	22.90	22.88	68.6	47.8	66.2
Mean:	**1186.8**	**1175.3**	**298.7**	**448.7**	**31.8**	**0.9**	**19.1**	**0.6**	**19.7**	**21.4**	**75.0**	**47.3**	**62.9**
SEM:	**33.6**	**57.0**	**18.0**	**30.2**	**0.5**	**0.0**	**0.9**	**0.0**	**0.9**	**0.6**	**3.4**	**4.2**	**5.5**

PEG														
Animal	Group	Mass: Surgery (g)	Mass: FM (g)	Defect Mass (mg)	Def LGAS Mass (mg)	Def MGAS Mass (mg)	Def SOL Mass (mg)	Def PLAN Mass (mg)	Def LGAS Length (mm)	Def LGAS CSA (cm^2)	Def Tetanic Force (N)	Optimal Length (N)	Def Max Force (N)	Def Specific Tension (N/cm^2)
201	ECM+PEG	636	609	318	1449	1337	249	560	33	1.08	11.20	0.60	11.80	10.91
202	ECM+PEG	648	632	300	1060	1438	304	543	31	0.84	8.30	0.60	8.90	10.56
203	ECM+PEG	600	598	330	1282	1391	299	496	32	0.99	13.90	0.60	14.50	14.69
204	ECM+PEG	550	555	311	1084	1324	270	500	33	0.81	7.05	0.55	7.60	9.39
205	ECM+PEG	560	585	303	1050	1353	283	528	33	0.78	7.10	0.50	7.60	9.69
Mean:		**598.8**	**595.8**	**312.4**	**1185.0**	**1368.6**	**281.0**	**525.4**	**32.4**	**0.9**	**9.5**	**0.6**	**10.1**	**11.0**
SEM:		**19.6**	**12.8**	**5.4**	**78.5**	**20.7**	**10.0**	**12.3**	**0.4**	**0.1**	**1.3**	**0.0**	**1.3**	**1.0**

PEG														
Animal	Con LGAS Mass (mg)	Con MGAS Mass (mg)	Con SOL Mass (mg)	Con PLAN Mass (mg)	Con LGAS Length (mm)	Con LGAS CSA (cm^2)	Def Tetanic Force (N)	Optimal Length (N)	Def Max Force (N)	Con Specific Tension (N/cm^2)	LGAS Mass (% Contralateral)	Def Force (% Contralateral)	Specific Tension (% Contralateral)	Def Specific Tension (N/cm^2)
201	1598	1241	323	542	33	1.19	22.4	0.60	23.00	19.28	90.7	50.0	56.6	10.91
202	1308	1403	300	490	33	0.98	18.95	0.55	19.50	19.97	81.0	43.8	52.9	10.56
203	1329	1356	304	459	33	0.99	20.8	0.60	21.40	21.57	96.5	66.8	68.1	14.69
204	1375	1170	252	465	32	1.06	20.7	0.60	21.30	20.12	78.8	34.1	46.7	9.39
205	1118	1466	256	442	32	0.86	16.55	0.55	17.10	19.86	93.9	42.9	48.8	9.69
Mean:	**1345.6**	**1327.2**	**287.0**	**479.6**	**32.6**	**1.0**	**19.9**	**0.6**	**20.5**	**20.2**	**88.2**	**47.5**	**54.6**	**11.0**
SEM:	**76.8**	**53.8**	**14.0**	**17.4**	**0.2**	**0.1**	**1.0**	**0.0**	**1.0**	**0.4**	**3.5**	**5.5**	**3.8**	**1.0**

PEGMSC													
Animal	Con LGAS Mass (mg)	Con MGAS Mass (mg)	Con SOL Mass (mg)	Con PLAN Mass (mg)	Con LGAS Length (mm)	Con LGAS CSA (cm^2)	Def Tetanic Force (N)	Optimal Length (N)	Def Max Force (N)	Con Specific Tension (N/cm^2)	LGAS Mass (% Contralateral)	Def Force (% Contralateral)	Specific Tension (% Contralateral)
	1379	1176	242	509	31	1.10	21.70	0.60	21.30	19.43	73.7	46.1	69.7
301	1185	1027	272	423	32	0.91	18.40	0.60	19.00	20.82	81.9	52.2	67.6
302	1306	1217	288	461	32	1.01	18.80	0.60	19.40	19.29	77.2	49.5	68.2
304	1307	1163	273	450	33	0.98	16.85	0.55	17.40	17.83	72.7	44.5	69.0
305	1207	998	240	402	33.5	0.89	19.60	0.60	20.20	22.75	70.4	66.8	94.2
Mean:	**1276.8**	**1116.2**	**263.0**	**449.0**	**32.3**	**1.0**	**19.1**	**0.6**	**19.5**	**20.0**	**75.2**	**51.8**	**73.7**
SEM:	**35.7**	**43.5**	**9.4**	**18.2**	**0.4**	**0.0**	**0.8**	**0.0**	**0.6**	**0.8**	**2.0**	**4.0**	**5.1**

NERVE GROUP				***Defect (Left) Leg***										
Animal	Group	Mass: Surgery (g)	Mass: FM (g)	Defect Mass (mg)	Def LGAS Mass (mg)	Def MGAS Mass (mg)	Def SOL Mass (mg)	Def PLAN Mass (mg)	Def LGAS Length (mm)	Def LGAS CSA (cm^2)	Def Tetanic Force (N)	Optimal Length (N)	Def Max Force (N)	Def Specific Tension (N/cm^2)
401	nerve	474	469	285	772	870	315	369	32	0.59	6.20	0.60	6.80	11.44
402		500	489	290	765	1103	277	475	32	0.59	10.65	0.55	11.20	19.01
403		571	550	335	1030	1120	257	474	31	0.82	12.80	0.60	13.40	16.37
404		628	636	309	1277	1353	318	548	31	1.01	18.60	0.60	19.00	18.72
405		601	640	309	1055	1310	292	564	32	0.81	9.80	0.60	10.40	12.80
										---				---
Mean:		**554.8**	**556.8**	**305.6**	**979.8**	**1151.2**	**291.8**	**486.0**	**31.6**	**0.8**	**11.6**	**0.6**	**12.2**	**15.7**
SEM:		**29.4**	**35.7**	**8.8**	**96.4**	**86.1**	**11.5**	**34.6**	**0.2**	**0.1**	**2.0**	**0.0**	**2.0**	**1.5**

NERVE GROUP	***Contralateral/Control (Right) Leg***												
Animal	Con LGAS Mass (mg)	Con MGAS Mass (mg)	Con SOL Mass (mg)	Con PLAN Mass (mg)	Con LGAS Length (mm)	Con LGAS CSA (cm^2)	Def Tetanic Force (N)	Optimal Length (N)	Def Max Force (N)	Con Specific Tension (N/cm^2)	LGAS Mass (% Contralateral)	Def Force (% Contralateral)	Specific Tension (% Contralateral)
401	1236				32	0.95	16.50	0.60	17.10	17.97	62.5	37.6	63.7
402	1106				32	0.85	18.35	0.55	18.90	22.19	69.2	58.0	85.7
403	1129	1142	241	438	31	0.90	19.20	0.60	19.80	22.07	91.2	66.7	74.2
404	1307	1493	374	495	32	1.01	21.30	0.60	21.90	21.76	97.7	87.3	86.0
405	1061	1344	232	477	35	0.75	13.80	0.50	14.30	19.15	99.4	71.0	66.9
						---				---			
Mean:	**1167.8**	**1326.3**	**282.3**	**470.0**	**32.4**	**0.9**	**17.8**	**0.6**	**18.4**	**20.6**	**84.0**	**64.1**	**75.3**
SEM:	**45.1**	**101.7**	**45.9**	**16.8**	**0.7**	**0.0**	**1.3**	**0.0**	**1.3**	**0.9**	**7.6**	**8.2**	**4.6**

NERVEPEG			Defect (Left) Leg					
Animal	Mass: Surgery (g)	Mass: FM (g)	Defect Mass (mg)	Def LGAS Mass (mg)	Def MGAS Mass (mg)	Def SOL Mass (mg)	Def PLAN Mass (mg)	Def LGAS Length (mm)
501	684	723	294	999	1220	300	440	31
502	592	595	304	1107	1323	204	495	30
504	587	633	317	1144	1193	262	535	35
505	537	558	326	1305	1398	321	600	33
506	583	614	324	1278	1375	268	468	34
Mean:	**596.6**	**624.6**	**313.0**	**1166.6**	**1301.8**	**271.0**	**507.6**	**32.6**
SEM:	**24.0**	**27.5**	**6.1**	**56.4**	**41.0**	**19.9**	**27.9**	**0.9**

NERVEPEG			DefContralateral/Control (Right) Leg							
Animal	Con PLAN Mass (mg)	Con LGAS Length (mm)	Con LGAS CSA (cm^2)	Def Tetanic Force (N)	Optimal Length (N)	Def Max Force (N)	Con Specific Tension (N/cm^2)	LGAS Mass (% Contralateral)	Def Force (% Contralateral)	Specific Tension (% Contralateral)
501	381	33	0.90	18.80	0.60	19.40	21.65	83.3	41.5	48.9
502	466	32	1.02	19.10	0.60	19.70	19.22	83.2	49.2	53.8
504	420	35	1.03	18.20	0.60	18.70	18.22	78.5	49.5	65.4
505	426	32	1.07	19.90	0.60	20.50	19.07	93.5	54.0	60.8
506	441	34	1.02	20.05	0.55	20.60	20.16	90.6	49.9	56.8
			---				---			
Mean:	**426.8**	**33.2**	**1.0**	**19.2**	**0.6**	**19.8**	**19.7**	**85.8**	**48.8**	**57.1**
SEM:	**13.9**	**0.6**	**0.0**	**0.3**	**0.0**	**0.4**	**0.6**	**2.7**	**2.0**	**2.8**

NERVEPEG			DefContralateral/Control (Right) Leg							
Animal	Con PLAN Mass (mg)	Con LGAS Length (mm)	Con LGAS CSA (cm^2)	Def Tetanic Force (N)	Optimal Length (N)	Def Max Force (N)	Con Specific Tension (N/cm^2)	LGAS Mass (% Contralateral)	Def Force (% Contralateral)	Specific Tension (% Contralateral)
501	381	33	0.90	18.80	0.60	19.40	21.65	83.3	41.5	48.9
502	466	32	1.02	19.10	0.60	19.70	19.22	83.2	49.2	53.8
504	420	35	1.03	18.20	0.60	18.70	18.22	78.5	49.5	65.4
505	426	32	1.07	19.90	0.60	20.50	19.07	93.5	54.0	60.8
506	441	34	1.02	20.05	0.55	20.60	20.16	90.6	49.9	56.8
			---				---			
Mean:	**426.8**	**33.2**	**1.0**	**19.2**	**0.6**	**19.8**	**19.7**	**85.8**	**48.8**	**57.1**
SEM:	**13.9**	**0.6**	**0.0**	**0.3**	**0.0**	**0.4**	**0.6**	**2.7**	**2.0**	**2.8**

NERVEPEGMSC			Defect (Left) Leg							
Animal	Mass: Surgery (g)	Mass: FM (g)	Defect Mass (mg)	Def LGAS Mass (mg)	Def MGAS Mass (mg)	Def SOL Mass (mg)	Def PLAN Mass (mg)	Def LGAS Length (mm)	Def LGAS CSA (cm^2)	Def Tetanic Force (N)
601	532	550	302	806	1206	218	441	34	0.58	7.90
602	477	503	321	1245	1286	232	496	33	0.93	17.80
603	547	624	295	1040	1471	448	617	34	0.75	8.65
604	405	396	309	808	1010	187	399	32	0.62	7.95
605	563	620	301	1079	1355	272	539	34	0.78	20.65
Mean:	**504.8**	**538.6**	**305.6**	**995.6**	**1265.6**	**271.4**	**498.4**	**33.4**	**0.7**	**12.6**
SEM:	**28.8**	**42.2**	**4.4**	**84.3**	**77.3**	**46.2**	**38.0**	**0.4**	**0.1**	**2.7**

NERVEPEGMSC				Contralateral/Control (Right) Leg						
Animal	Optimal Length (N)	Def Max Force (N)	Def Specific Tension (N/cm^2)	Con LGAS Mass (mg)	Con MGAS Mass (mg)	Con SOL Mass (mg)	Con PLAN Mass (mg)	Con LGAS Length (mm)	Con LGAS CSA (cm^2)	Def Tetanic Force (N)
601	0.50	8.40	14.38	1178	1134	224	360	33	0.88	15.65
602	0.60	18.40	19.79	1320	1155	230	423	33	0.99	21.00
603	0.55	9.20	12.21	1424	1296	301	468	33	1.06	16.30
604	0.55	8.50	13.66	1045	820	208	314	31	0.83	13.95
605	0.55	21.20	27.11	1226	978	243	397	35	0.86	21.60
Mean:	**0.6**	**13.1**	**17.4**	**1238.6**	**1076.6**	**241.2**	**392.4**	**33.0**	**0.9**	**17.7**
SEM:	**0.0**	**2.8**	**2.7**	**64.2**	**81.6**	**16.0**	**26.3**	**0.6**	**0.0**	**1.5**

NERVEPEGMSC						
Animal	Optimal Length (N)	Def Max Force (N)	Con Specific Tension (N/cm^2)	LGAS Mass (% Contralateral)	Def Force (% Contralateral)	Specific Tension (% Contralateral)
601	0.55	16.20	18.42	68.4	50.5	78.1
602	0.60	21.60	21.92	94.3	84.8	90.3
603	0.60	16.90	15.90	73.0	53.1	76.8
604	0.55	14.40	17.34	77.3	57.0	78.8
605	0.60	21.80	25.26	88.0	95.6	107.3
Mean:	**0.6**	**18.2**	**19.8**	**80.2**	**68.2**	**86.3**
SEM:	**0.0**	**1.5**	**1.7**	**4.8**	**9.2**	**5.8**

CROSS SECTIONAL AREA

Bottom

MYOFIBER SIZE	ECM	PEG	PEG+MSC	Nerve	Nerve+PEG	Nerve+PEG+MSC
500	24.90	19.77	18.08	32.61	15.14	15.73
1000	27.40	28.40	14.62	25.57	14.85	18.96
1500	15.53	14.04	7.45	11.33	6.35	10.92
2000	8.74	6.23	4.68	6.11	5.77	7.05
2500	4.55	3.07	4.82	4.31	4.22	4.76
3000	2.47	2.77	5.36	3.62	3.83	3.32
3500	2.04	2.60	6.19	3.60	3.10	2.68
4000	1.12	2.98	5.07	2.75	4.12	3.07
4500	1.55	2.75	4.38	2.64	4.22	2.92
5000	0.65	2.36	4.38	1.74	3.68	2.53
5500	0.92	2.77	3.46	1.45	3.88	3.27
6000	1.08	2.80	4.53	1.13	5.09	3.07
6500	0.82	2.13	3.70	0.97	4.41	2.73
7000	0.65	1.84	2.19	0.79	4.36	2.33
7500	0.95	1.22	2.09	0.45	4.07	3.32
>7500	6.56	4.18	8.92	0.84	12.81	13.25
% OF AVERAGE:	6.16	15.82	25.54	10.72	25.43	17.62
SEM:	1.25	1.29	2.38	3.08	2.00	1.09

Middle

MYOFIBER SIZE	ECM	PEG	PEG+MSC	Nerve	Nerve+PEG	Nerve+PEG+MSC
500	26.51	25.85	15.86	14.70	16.56	15.14
1000	33.58	29.33	26.09	16.00	27.38	22.58
1500	17.23	15.82	15.29	13.28	16.82	17.24
2000	7.39	8.23	8.91	8.78	10.01	11.95
2500	4.38	4.41	5.66	8.67	6.20	7.05
3000	2.96	3.09	3.99	7.13	4.53	4.34
3500	1.64	2.91	3.27	6.34	3.98	3.57
4000	1.25	2.15	2.74	3.62	2.68	3.66
4500	0.99	1.63	2.45	3.90	1.96	2.24
5000	0.64	1.45	2.56	2.91	1.47	2.15
5500	0.74	1.16	1.96	2.99	1.58	1.71
6000	0.51	0.80	1.78	2.08	1.18	1.44

6500	0.39	0.64	0.99	1.77	0.69	1.06
7000	0.53	0.57	1.28	1.22	0.69	0.97
7500	0.18	0.38	1.24	1.18	0.60	0.79
>7500	0.99	1.48	5.84	5.36	3.60	4.04
% OF AVERAGE:	4.54	7.87	12.51	17.30	9.58	12.28
SEM:	1.30	2.27	2.64	3.39	2.78	3.69

Top

MYOFIBER SIZE	**ECM**	**PEG**	**PEG+MSC**	**Nerve**	**Nerve+PEG**	**Nerve+PEG+MSC**
500	11.74	16.15	8.01	14.02	21.49	13.81
1000	19.29	17.00	18.31	18.14	19.60	17.84
1500	14.69	11.50	13.16	12.95	10.93	11.52
2000	10.79	9.34	8.49	10.34	8.16	8.78
2500	8.12	7.86	5.30	7.17	6.07	6.40
3000	6.87	5.66	5.20	6.55	4.35	5.03
3500	4.70	5.03	3.92	5.15	4.45	4.91
4000	3.75	3.59	3.29	3.42	4.35	4.14
4500	2.91	4.06	3.07	3.31	3.71	5.23
5000	2.87	2.45	2.86	3.23	3.34	4.02
5500	2.23	2.41	3.34	2.28	2.42	3.10
6000	1.92	1.77	2.81	1.58	1.61	1.89
6500	2.20	1.43	2.86	1.65	1.78	1.77
7000	1.15	1.69	2.38	1.54	1.85	2.05
7500	1.42	1.52	2.33	1.32	1.11	1.57
>7500	5.28	8.46	14.59	7.28	4.69	7.85
% Average :	15.91	15.73	18.25	15.49	17.24	20.18
SEM:	2.73	4.166	0.9462	3.47	4.49	5.57

BLOOD VESSEL DENSITY

		Total Defect Count			Bold Vessel Density (BV/mm²)		
	Saline	ECM Region					
Animal	Region within Region	Top	Middle	Botom	Top	Middle	Bottom
103	Top	4	5	2	6.11	6.67	8
	Middle	3	4	6			
	Bottom	4	3	4			
101	Top	3	6	6	4.44	9.44	11.33
	Middle	2	6	4			
	Bottom	3	5	7			
106	Top	5	5	4	7.22	6.11	11.33
	Middle	3	3	6			
	Bottom	5	3	7			
				Average:	5.93	7.40	10.22
				SEM:	0.81	1.03	1.11
206	Top	4	5	10	11.11	8.33	17.33
	Middle	7	5	7			
	Bottom	9	5	9			
203	Top	3	6	8	10.56	9.44	16
	Middle	6	6	9			
	Bottom	10	5	7			
				Average:	10.83	8.89	16.67
				SEM:	0.28	0.56	0.67
301	Top	6	4	10	10	11.67	12.67
	Middle	6	10	6			
	Bottom	6	7	3			
302	Top	5	9	10	9.44	12.22	13.33
	Middle	6	7	6			
	Bottom	6	6	4			
304	Top	5	8	7	13.33	12.78	16.67
	Middle	9	8	9			
	Bottom	10	9	9			
				Average:	10.93	12.22	14.22
				SEM:	1.21	0.32	1.24

402	Top	14	16	9	15.56	22.22	15.33
	Middle	6	15	6			
	Bottom	8	9	8			
403	Top	11	5	3	14.44	8.33	9.33
	Middle	10	6	5			
	Bottom	5	4	6			
407	Top	5	11	6	9.44	16.67	10
	Middle	6	12	2			
	Bottom	6	7	7			
				Average:	13.14	15.74	11.56
				SEM:	1.87	4.03	1.89
500	Top	8	8	12	17.78	16.67	24
	Middle	12	10	10			
	Bottom	12	12	14			
503	Top	7	8	8	11.67	11.67	14
	Middle	8	6	8			
	Bottom	6	7	5			
				Average:	9.81	9.44	12.67
				SEM:	1.03	2.76	4.07
602	Top	7	14	9	17.78	17.78	14.67
	Middle	14	9	6			
	Bottom	11	9	7			
603	Top	11	15	14	21.12	27.22	25.33
	Middle	12	19	10			
	Bottom	15	15	14			
604	Top	14	14	12	18.33	21.11	28
	Middle	7	12	16			
	Bottom	12	12	14			
				Average:	19.07	22.04	22.67
				SEM:	1.19	1.52	1.45

REFERENCES

Agrawal, V., Brown, B.N., Beattie, A.J. Gilbert, T.W., and Badylak S.F. (2009). Evidence of innervation following extracellular matrix scaffold mediated remodeling of muscular tissue. J Tissue Eng Regen. 3(8): 590-600.

Al-Khaldi, A., Eliopoulos, N., Martineau, D., Lejeune, L., Lachapelle, K., and Galipeau, J. (2003). Postnatal bone marrow stromal cells elicit a potent VEGF-dependent neoangiogenic response in vivo. *Gene Therapy*, 10: 621-629.

Armstrong, S.J., Wiberg, M., Terenghi, G., and Kingham, P.J. (2007). ECM molecules mediate both Schwann cell proliferation and activation to enhance neurite outgrowth. *Tissue Engineering.* 13 (12): 2863-2870.

Arnold, L., Henry, A., Poron, F., Baba-Amer, Y., Van Rooijen, N., Plonquet, A., Gherardi, R.K., Chazaud, B. (2007). Inflammatory monocytes recruited after skeletal muscle injury switch into antiinflammatory macrophages to support myogenesis. *Journal of Experimental Medicine, 204*(5), 1057-1069.

Autiero, M., De Smet, F., Claes, F., and Carmeliet, P. (2005). Role of neural guidance signals in blood vessel navigation. *Cardiovascular Research,* 65: 629-638.

Badylak, S.F., Park, K., Peppas, N., Mccabe, G.P., and Yoder, M**.** (2001). Marrow-derived cells populate scaffolds composed of xenogeneic extracellular matrix. *Experimental Hematology, 29* (11):1310-1318.

Badylak, S., Obermiller, J., Geddes, L., & Matheny, R. (2003). Extracellular matrix for myocardial repair. *Heart Surg Forum, 6*(2), E20-26.

Badylak, S.F. (2004). Xenogeneic extracellular matrix as a scaffold for tissue reconstruction. *Transplant Immunology,* 12 (3–4): 367–377.

Badylak, S.F. (2007). The extracellular matrix as a biologic scaffold material. *Biomaterials,* 28: 3587–3593

Badylak, S.F., and Gilbert T.W. (2008). Immune response to biologic scaffold materials**.** *Seminars in Immunology,* 20 (2): 109–116.

Badylak, S.F. (2008). Biologic scaffold materials for orthopaedic soft tissue reconstruction. Musculoskeletal Tissue Regeneration, 443-457.

Badylak, S. F., Valentin, J. E., Ravindra, A. K., McCabe, G. P., & Stewart-Akers, A. M. (2008). Macrophage phenotype as a determinant of biologic scaffold remodeling. *Tissue Engineering Part A, 14*(11), 1835-1842.

Badylak, S.F., Beattie, A.J., Gilbert, T.W., Guyot, J.P.. and Yates, A. J. (2009). Chemoattraction of progenitor cells by remodeling extracellular matrix scaffolds. *Tissue Engineering, Part A: Tissue Engineering.* 15.5: 1119

Badylak, S.F., Freytes D.O., and Gilbert T.W. (2009). Extracellular matrix as a biological scaffold material: structure and function. *Acta Biomaterialia,* 5 (1): 1-13.

Belmont PJ, Schoenfeld AJ, Goodman G. (2010). Epidemiology of combat wounds in Operation Iraqi Freedom and Operation Enduring Freedom: orthopedic burden of disease. *Surg Orthop Adv,* 19 (1): 2-7.

Bixby J.L., and Van Essen, D.C. (1979). Competition between foreign and original nerves in adult mammalian skeletal muscle. *Nature*, 282: 726-729.

Borschel, G. H., Dennis, R. G., & Kuzon, W. M. (2004). Contractile Skeletal Muscle Tissue-Engineered on an Acellular Scaffold. *Plastic and Reconstructive Surgery, 113*(2), 595-602.

Borisov AB, Dedkov EI, Carlson BM. (2001) Interrelations of myogenic response, progressive atrophy of muscle fibers, and cell death in denervated skeletal muscle. *Anatomical Record*, 264: 203-218.

Borisov AB, Dedkov EI, and Carlson BM. (2005) Abortive myogenesis in denervated skeletal muscle: differentiative properties of satellite cells, their migration, and block of terminal differentiation. *Anatomical Embryology*, 209: 269-279.

Brown, B.N., Valentin, J.E., Stewart-Akers, A.M, McCabe, G.P., and Badylak, S.F. (2009). Macrophage phenotype and remodeling outcomes in response to biologic scaffolds with and without a cellular component. *Biomaterials,* 30 (8). 1482-1491.

Brown, B.N., and Badylak, S.F. (2014). Extracellular matrix as an inductive scaffold for functional tissue reconstruction. *Translational Research,* 163 (4): 268–285.

Calza, L., Giardino, L., Giuliani, A., Aloe, L., and Levi-Montalcini. (2001). Nerve growth factor control of neuronal expression of angiogenetic and vasoactive factors. *Proceedings of the National Academy of Sciences of the United States of America,*98 (7):4160-4165.

Carlson, B.M., and Faulkner, J.A. (1983). The regeneration of skeletal muscle fibers following injury: a review. *Medicine and Science in Sports and Exercise,* 15 (3): 187-198.

Charge, S.B, and Rudnicki, M.A. (2004). Cellular and molecular regulation of muscle regeneration. *Physiology Review,* 84: 209-238.

Chazaud, B., Brigitte, M., Yacoub-Youssef, H., Arnold, L., Gheraldi, R., Sonnet, C., Lafuste, P. and Chretien, F. (2008). Dual and beneficial roles of macrophages during skeletal muscle regeneration. *Exercise and Sports Science Reviews,* 37 (1): 18-22.

Christov, C., Chretien, F., Abou-Khalil, R., Bassez, G., Vallet, G., Authier, F., Bassaglia, Y., Shinin, V., Tajbakhsh, S., Chazaud, B., and Gherardi, R.K. (2007). Muscle satellite cells and endothelial cells: close neighbors and privileged partners. *Molecular Biology of the Cell.* 18:1397-1409.

Clow, C. and Jasmin, B.J. (2010). Brain-derived neurtrophic factor regulates satellite cell differentiation and skeletal muscle regeneration. *The American Society of Cell Biology,* 21: 2182-2190.

Collins, C.A., Olsen, I., Zammit, P.S., Heslop, L., Petrie, A., Partridge, T.A., and Morgan, J.E. (2005). Stem cell function, self-renewal, and behavioral heterogeneity of cells from the adult muscle satellite cell niche. *Cell,* 122: 289-301.

Collins, C.A., and Partridge, T.A. (2005). Self-renewal of the adult skeletal muscle satellite cell. *Cell Cycle,* 4 (10): 1338-1341.

Conboy, I.M., Conboy, M.J., Wagers, A.J., Girma, E.R., Weissman, I.L. and Rando, T.A. (2005). Rejuvination of aged progenitor cells by exposure to a young systemic environment. *Nature,* 433: 760-764.

Dhawan, V., Lytle, I.F., Dow, D.E., Huang, Y., and Brown, D.L. (2007). Neurotization improves contractile forces of tissue-engineered skeletal muscle. *Tissue Engineering,* 13 (11):2813- 2821.

Dezawa, M., Ishikawa, H., Itokazu, Y., Yoshihara, T., Hoshino, M., Takeda, S., Ide, C., Nabeshima, Y. (2005). Bone marrow stromal cells generate muscle cells and repair muscle degeneration. *Science*, 309: 314-317.

Drinnan, C.T., Zhang, G., Alexander, M.A., Pulido, A.S., and Suggs, L.J. (2010). Multimodal release of transforming growth factor-β1 and the BB isoform of platelet derived growth factor from PEGylated fibrin gels. *Journal of Controlled Release.* 147:180-186.

Emanueli, C., Salis, M.B., Pinna, A., Graiani, G., Manni, L., and Madeddu, P. (2002). Nerve growth factor promotes angiogenesis and arteriogenesis in ischemic hindlimbs. *Circulation,* 106:2257-2262.

Fan, C., Jang, P., Fu, L., Cai, P., Sun, L., and Zeng, B. (2008). Functional reconstruction of traumatic loss of flexors in forearm with gastrocnemius myocutaneous flap transfer. *Microsurgery,* 28L: 71.

Friedenstein, A. J., Chailakhyan, R. K., Latsinik, N. V., Panasyuk, A. F., & Keiliss-Borok, I. V. (1974). Stromal cells responsible for transferring the microenvironment of the hemopoietic tissues. Cloning in vitro and retransplantation in vivo. *Transplantation, 17*(4), 331-340.

Gherardi, R. K., and Chazaud, B. (2007). Inflammatory monocytes recruited after skeletal muscle injury switch into antiinflammatory macrophages to support myogenesis. *Journal of Experimental Medicine,* 204(5): 1057–1069.

Gilbert, P.M., Havenstrite, K.L., Magnusson, K.E.G., Sacco, A., Leonardi, N.A., Kraft, P., Nguyen, N.K., Thrun, S., Lutolf, M.P., and Blau, H.M. (2010). Substrate elasticity regulates skeletal muscle stem cell self-renewal in culture. *Science,* 329:1078-1081.

Gimbel, J.M., Floyd, Z.E., and Bunnell, B.A. (2009). The 4th dimension and adult stem cells: can timing be everything. *Journal of Cellular Biochemistry,*107 (4): 569-578.

Gonzalez-Perez, F., Udina, E., and Navarro, X. (2013). Extracellular matrix components in peripheral nerve regeneration. *International Review of Neurobiology,* 108: 257-275.

Grogan, B.F., and Hsu, J.R. (2011). Volumetric muscle loss. *Journal of the American Academy of Orthopaedic Surgeons,* 19 (S1): S35-S37.

Gussoni, E., Soneoka, Y., Strickland, C.D., Buzney, E.A., Khan, M., Flint, A.F., Kunkel, L.M., and Mulligan, R.C. (1999). Dystrophin expression in the *mdx* mouse restored by stem cell transplantation. *Naure* 401(23): 390-393.

Hammers, D.W., Sarathy, A., Pham, C.B., Drinnan, C.T., Farrar, R.P., and Suggs, LJ. (2012). Controlled release of IGF-I from a biodegradable matrix improves functional recovery of skeletal muscle from ischemia/reperfusion. *Biotechnology and Bioengineering,* 109(4): 1051-1059.

Hill, M., Wernig, A., and Goldspink, G. (2003). Muscle satellite (stem) cell activation during local tissue injury and repair. *Journal of Anatomy,* 203: 89-99.

Hinds, S., Bian, W., Dennis, R.G., and Bursac, N. (2011). The role of extracellular matrix composition in structure and function of bioengineered skeletal muscle. *Biomaterials.* 32: 3575-3583.

Hirata, M., Sakuma, K., Okajima, S., Fujiwara, H., Inashima, S., Yasuhara, M., and Kubo, T. (2007). Increased expression of neuregulin-1 in differentiatiaon muscle satellite cells and in motoneurons during muscle regeneration. *Acta Neuropathologogy,* 113: 452-459.

Hollister, S.J. (2005). Porous scaffold design for tissue engineering. *Nature Materials,* 4: 518-524.

Huard, J., Li, Y., and Fu, F. (2002). Muscle injuries and repair: current trends in research. *Journal of Bone and Joint Surgery, 84A*(5), 822-832.
Huntsman, H.D., Zachwieja, N., Zou, K., Ripchik, P.,Valero, M.C., De Lisio, M., and Boppart, M.D. (2103). Mesenchymal stem cells contribute to vascular growth in skeletal muscle in response to eccentric exercise. *Am J Physiol Heart Circ Physiol,* 304:H72-H81.

Jacobson, C., Duggan, D., and Fischbach, G. (2004). Neuregulin induces the expression of transcription factors and myosin heavy chains typical of muscle spindles in cultured human muscle. *Proceedings of the National Academy of Sciences of the United States of America,* 101(33): 12218-12223.

Jarvinen, M. (1976a). Healing of a crush injury in rat striated muscle. 3. A micro-angiographical study of the effect of early mobilization and immobilization on capillary ingrowth. *Acta Pathol Microbiol Scand A, 84*(1), 85-94.

Jarvinen, T., Jarvinen, T., Kaariainen, M., Kalimo, H., and Jarvinen, M. (2005). Muscle injuries: biology and treatment. *American Journal of Sports Medicine, 33*(5), 745-764.

Jarvinen, T., Jarvinen, T., Kaariainen, Aarima, V., Vaittinen, S., M., Kalimo, H., and Jarvinen, M. (2007). Muscle injuries: optimising recovery. *Best Practice & Research Clinical Rheumatology,* 21(2), 317-331.

Jarvinen, T.A, Kaariainen, M., Aarimaa, V., Jarvinen, M., and Kalimo, H. (2008). Skeletal muscle repair after exercise-induced injury. In *Skeletal Muscle repair and Regeneration. Advances in Muscle Research,* Ch 11. 217-242.

Juhas, M., and Bursac, N. (2013). Engineering skeletal muscle repair. *Current Opinion in Biotechnology*, 24:880–886.

Kaariainen, M., Kaariainen, J., Jarvinen, T. L., Nissinen, L., Heino, J., Jarvinen, M., and Kalimo, H. (2000). Integrin and dystrophin associated adhesion protein complexes during regeneration of shearing-type muscle injury. *Neuromuscular Disorders, 10*(2), 121-132.

Kang, H., Tian, L., and Thompson, W.J. (2003). Terminal Schwann cells guide the reinnervation of muscle after nerve injury. *Journal of Neurocytology.* 32: 975-985.

Karpati, G and Molnar, M.J (2008). Muscle Fibre Regeneration in Human Skeletal Muscle Diseases. In *Skeletal Muscle repair and Regeneration. Advances in Muscle Research 3,* Ch 10. 199-216.

Keilhoff,G., Goihl, A., Stang, F., Wolf, G., and Fansa, H. (2006). Peripheral nerve tissue engineering: autologous Schwann cells vs. transdifferentiated mesenchymal stem cells. *Tissue Engineering, 1* 2(6): 1451-1465.

Kopp, D.M., Trachtenberg, J.T., and Thompson, W.J. (1997). Glial growth factor rescues Schwann Cells of mechanoreceptors from denervation-induced apoptosis. *The Journal of Neuroscience,* 17(17): 6697-6706.

Kragh, J. F., Svoboda, S. J., Wenke, J. C., Ward, J. A., & Walters, T. J. (2005). Epimysium and Perimysium in Suturing in Skeletal Muscle Lacerations. *The Journal of Trauma: Injury, Infection, and Critical Care, 59*(1), 209-212.

Kuang, S., Gillespie, M.A., and Rudnicki, M.A. (2008). Niche regulation of muscle satellite cell self-renewal and differentiation. *Cell Stem Cell Review,* 2: 22-31.

LaBarge, M. A., & Blau, H. M. (2002). Biological progression from adult bone marrow to mononucleate muscle stem cell to multinucleate muscle fiber in response to injury, *Cell, 111*(4), 589-601.

Lavasani, M., Lu, A., Peng, H., Cummins, J. and Huard, J. (2006). Nerve growth factor improves the muscle regeneration capacity of muscle stem cells in dystrophic muscle. *Human Gene Therapy,* 17:180-192.

Lee, R. H., Pulin, A.A., Seo, M.J., Kota, D.J., Ylostalo, J., Larson, B.L., Semprun-Prieto, L., Delafontaine, P., and Prockop, D.J. (2009). Intravenous hMSCs improve myocardial infarction in mice because cells embolized in lung are activated to secrete the anti-inflammatory protein TSG-6. *Cell Stem Cell,* 5(1): 54-63.

Li, G.N., Livi, L.I., Gourd, C.M., Deweerd, E.S., and Hoffman-Kim, D. (2007). Genomic and morphological changes of neuroblastoma cells in response to three-dimensional matrices. *Tissue Engineering,* 13:1035-1047.

Li, M.T.A., Willett, N.J., Uhrig, B.A., Guldberg, R.E., and Warren, G.L. (2013*)*. Functional analysis of limb recovery following autograft treatment of volumetric muscle loss in the quadriceps femoris. *Journal of Biomechanics,* 47: 2013–2021.

Lolmede, K., Campana, L., Vezzoli, M., Bosurgi, L., Tonlorenzi, R., Clementi, E., . . . Rovere-Querini, P. (2009). Inflammatory and alternatively activated human macrophages attract vessel-associated stem cells, relying on separate HMGB1- and MMP-9-dependent pathways. *Journal of Leukocyte Biology, 85*(5), 779-787.

Love, F.M., and Thomspon, W.J. (1998). Schwann cells proliferate at rat neuromuscular junctions during development and regeneration. *The Journal of Neuroscience,* 18 (22): 9376-9385.

Madaghiele, M., Sannino, A., Yannas, I.V., and Spector, M. (2007). Collagen-based matrices with axially oriented pores. *Journal of Biomedical Materials Research Part,* 85A: 757-767.

Martin, B.J., Senechal, G., and Pittenger, M.F. (1999). Implantation and myogenic differentiation of human mesenchymal stem cells in infracted rat myocardium. *Journal of Cardiac Failure,* 5 (3): 2.

Mase Jr., V.J., Hsu, J.R., Wolf, S.E.,Wenke, J.C., Baer, D. G., Owens, J., Badylak, S.F., and Walters, T.J. (2010). Clinical application of an acellular biologic scaffold for surgical repair of a large, traumatic quadriceps femoris muscle defect. *Orthopedics,* 33 (7). 511.

Masini, B.D., Waterman, S.M., Wenke, J.C., Owens, B.D., Hsu JR, and Ficke, J.R. (2009). Resource utilization and disability outcome assessment of combat casualties from Operation Iraqi Freedom and Operation Enduring Freedom. *Journal of Orthapedic Trauma,* 23 (4): 261 – 266.

Matthes, S.M., Reimers, K., Janssen, I., Leibsch, C., Kocsis, J.D., Vogt, P.M., and Radtke, C. (2013). Intravenous transplantation of mesenchymal stromal cells to enhance peripheral nerve regeneration. *Biome Research International.* 1-6.
Meintjes, J., Yan, S., Zheng, M., Zheng, S., and Zhou, L. (2011). Synthetic, biological and composite scaffolds for abdominal wall reconstruction. *Expert Review of Medical Devices, 8*(2), 275.

Merritt, E. K., Cannon, M. V., Hammers, D. W., Le, L. N., Gokhale, R., Sarathy, A., Song, T.J., Tierney, M.T., Suggs, L.J., Walters, T.J., and Farrar, R. P. (2010). Repair of traumatic skeletal muscle injury with bone-marrow-derived mesenchymal stem cells seeded on extracellular matrix. *Tissue Eng Part A, 16*(9), 2871-2881.

Merritt, E. K., Hammers, D. W., Tierney, M., Suggs, L. J., Walters, T. J., and Farrar, R. P. (2010). Functional Assessment of Skeletal Muscle Regeneration Utilizing Homologous Extracellular Matrix as Scaffolding. *Tissue Engineering Part A, 16*(4), 1395-1405.

Nehrer-Tairych, G.V., Rab, M., Kamolz, L., Deutinger, M., Stohr, H.G. and Frey, M. (2000). The influence of the donor nerve on the function and morpholofy of a mimic muscle after cross innervations: an experimental study in rabbits. *British Journal of Plastic Surgery,* 53 (8): 669-675.

Nisbet, D.R., Cropmton, K.E., Home, M.K., Finkelstein, D.I., and Forsythe, J.S. (2008). Neural tissue engineering of the CNS using hydrogels. *Journal of Biomedical Materials Research part B: Applied Biomaterials,* 87B:251-263.

Nitahara-Kasahara, Y., Hayashita-Kinoh, H., Ohshima-Hosoyama, S., Okada, H., Wada-Maeda, M., Nakamura, A., Okada, T., and Takeda, S. (2012). Long-term engraftment of multipotent mesenchymal stromal cells that differentiate to form myogenic cells in dogs with Duchenne muscular dystrophy. *Molecular Therapy.* 20 (1): 168-177.

Owens, B. D., Kragh, J. F., Macaitis, J., Svoboda, S. J., and Wenke, J. C. (2007). Characterization of Extremity Wounds in Operation Iraqi Freedom and Operation Enduring Freedom. *Journal of Orthopedic Trauma, 21*(4), 254-257.

Palermo, A.T., LaBarge, M.A., Doyonnas, R., Pomerantz, J., and Blau, H.M. (2005). Bone marrow contribution to skeletal muscle: a physiological response to stress. *Developmental Biology*, 279: 336-344.

Patzkowski J.C., Owens J.G., Blanck R.V., Kirk K.L., and Hsu J.R,. Skeletal Trauma Research Consortium (STReC). (2012). Deployment after limb salvage for high-energy lower-extremity trauma**.** *Journal Trauma Acute Care Surgery*, 73 (2 Suppl 1):S112-5.

Payne, S.H. and Brushart, T.M.(1997). Neurotization of the Rat soleus muscle: a quantitative analysis of reinnervation. *The Journal of Hand Surgery,* 22A: 640-643.

Pittenger, M. F., Mackay, A. M., Beck, S. C., Jaiswal, R. K., Douglas, R., Mosca, J. D., Moorman, M.A., Simonetti, D. W., Craig, S., and Marshak, D. R. (1999). Multilineage potential of adult human mesenchymal stem cells. *Science, 284*, 143-147.

Pittenger, M.F., and Martin, B.J. (2004). Mesenchymal stem cells and their potential as cardiac therapeutics. *Circulation Research,* 95: 9-20.

Prockop, D.J (2003) Further proof of the plasticity of adult stem cells and their role in tissue repair. *Journal of Cell Biology,* 160 (6): 807-809.

Prockop, D.J. (2009). Repair of tissues by adult stem/progenitor cells (MSCs): controversies, myths, and changing paradigms. *Molecular Therapy,* 1-8.

Qu, R., Li, Y., Gao, Q., Shen, L., Zhang, J., Liu, Z., Chen, X., and Chopp, M. (2007). Neurotrophic and growth factor gene expression profiling of mouse bone marrow stromal cells induced by ischemic brain extracts. *Neuropathology, 27*(4), 355-363.

Quintero, A. J., Wright, V. J., Fu, F. H., & Huard, J. (2009). Stem cells for the treatment of skeletal muscle injury. *Clinocal Sports Medicine, 28*(1), 1-11.

Rigamonti, E., Zordan, P., Sciorati, C., Rovere-Querini, P., and Brunelli, S. (2014).Macrophage Plasticity in Skeletal Muscle Repair. *BioMed Research International*,1-9.

Rippoll, C.B., and Bunnell, B.A. (2009). Comparitive characterization of mesenchymal stem cells from eGFP transgenic and non-transgenic mice. *BMC Cell Biology,* 10 (3): 1-12.

Sadat, S., Gehmert, S., Song, Y., Yen, Y., Bai, X., Gaiser, S., Klein, H., and Alt, E. (2007). The cardioprotective effect of mesenchymal stem cells is mediated by IGF-I and VEGF. *Biochemical and Biophysical Research Communications,* 363:674-679.

Schiaffano, S., and Partridge, T. (2008). Skeletal Muscle Repair and Regeneration. *Advances in Muscle Research 3, Vi-379.*

Schmidt, C.E. and Baier Leach, J. (2003). Neural tissue engineering: strategies for repair and regeneration. *Annual Review Biomedical Engineering,* 5: 293-347.

Schwander, M., Leu, M., Stumm, M., Dorchies, O.M., Ruegg, U.T., Schittny, J., and Muller, U. (2003). B1 integrins regulate myoblast fusion and sarcomere assembly. *Developmental Cell.* 4 (5): 673-685.

Schwander, M., Shiraski, R, Pfaff, S.L., And Muller, U. (2003). Beta1 integrins in muscle, but not in motor neurons, are required for skeletal muscle innervations. *Journal of Neuroscience.* 24 (37): 8181 – 8191.

Seal, A., and Stevanovich, M., (2011). Free functional muscle transfer for the upper extremety. *Clinical Plastic Surgery,* 38: 561-575.

Shabbir, A., Zisa, D., Leiker, M., Johnston, C., Lin, H., and Lee, T. (2009). Muscular dystrophy therapy by nonautologous mesenchymal stem cells: muscle regeneration without immunosuppression and inflammation. *Transplantation, 87*(9), 1275-1282.

Shimizu, S., Kitada, M., Ishikawa, H., Itokazu, Y., Wakao, S., and Dezawa, M. (2007). Peripheral nerve regeneration by the in vitro differentiatied-human bone marrow stromal cells with Schwann cell property. *Biochemical and Biophysical Research Communication.* 359: 915-920.

Sicari, B.M., Rubin, J.P., Dearth, C.L., Wolf, M.T., Ambrosio, F., Boninger, M., Turner, N.J., Weber, D.J., Simpson, T.W., Wyse, A., Brown, E.H.P., Dziki, J.L., Fisher, L.E. Brown, S., and Badylack S.F. (2014). An Acellular Biologic Scaffold Promotes Skeletal Muscle Formation in Mice and Humans with Volumetric Muscle Loss, *Science Translational Medicine, 6 (234).*

Singhal, N., and Martin, P. T. (2011). Role of the extracellular matrix protein and their receptors in the development of the vertebrate neuromuscular junction. *Developmental Neurobiology,* 71: 982-1005.

Son, Y., and Thompson, W.J. (1995). Schwann cell processes guide regeneration of peripheral axons. *Neuron,* 14: 125-132.

Son, Y., and Thompson, W.J. (1995). Nerve sprouting in muscle is induced and guided by processes extended by Schwann cells. *Neuron,* 14 (1):133-141.

Son, Y., Trachtenberg, J.T., Thompson, W.J. (1996). Schwann cells induce and guide sprouting and reinnervation of neuromuscular junctions. *Trends in Neuroscience,* 19: 280-285.

Stern, M. M., Myers, R. L., Hammam, N., Stern, K. A., Eberli, D., Kritchevsky, S. B., . . . Van Dyke, M. (2009). The influence of extracellular matrix derived from skeletal muscle tissue on the proliferation and differentiation of myogenic progenitor cells ex vivo. *Biomaterials, 30*(12), 2393-2399.

Sun, D., Shireman, P. K., Martinez, C. O., Ochoa, O., Ruiz-Willhite, L., Bonilla, J. R., Centonze, V. E., Waite, L.L., Michalek, J.E., and McManus, L.M. (2009). Bone marrow-derived cell regulation of skeletal muscle regeneration. *FASEB J, 23*(2), 382-395.

Tamaki,T., Uchiyama, Y., Okada, Y., Ishikawa, T., Sato, M., Akatsuka, A., and Asahara, T. (2005). Functional recovery of damaged skeletal muscle through synchronized vasculogenesis, myogenesis, and neurogenesis by muscle-derived stem cells. *Circulation,* 112: 2857-2866.

Tatsumi, R. (2010). Mechano-biology of skeletal muscle hypertrophy and regeneration: possible mechanism of stretch-induced activation of resident myogenic stem cells. *Animal Science Journal, 81*(1), 11-20.

Tedesco, F. S., Dellavalle, A., Diaz-Manera, J., Messina, G., & Cossu, G. (2010). Repairing skeletal muscle: regenerative potential of skeletal muscle stem cells. *Journal of Clinical Invest, 120*(1), 11-19.

Terada, N., Takayama, S., Yamada, H., and Seki, T. (2001). Muscle repair after a transsection injury with development of a gap: an experimental study in rats. *Scandavian Journal of Plasic Reconstruction & Hand Surgery, 35*: 233-238

Terada, N., Hamazaki, T., Oka, M., Hoki, M., Mastalerz, D.M., Nakano, Y., Meyer, E.M., Morel, L., Peterson, B.E., and Scott, E.W. (2002). Bone marrow cells adopt the phenotype of other cells by spontaneous cell fusion. *Nature*. 416: 542-545.

Tidball, J.G. (2005). Inflammatory processes in muscle injury and repair. *Am J Physiol Regul Integr Comp Physiol.* 288: R345-r353.

Trachtenberg, J.T. and Thompson, W.J. (1996). Schwann cell apoptosis at developing neuromuscular junctions is regulated by glial growth factor. *Nature,* 379: 174-177.

Trachtenberg, J.T. and Thompson, W.J. (1997). Nerve terminal withdrawal from rat neuromuscular junctions induced by neuregulin and Schwann cells. *The Journal of Neuroscience,* 17 (16): 6243-6255.

Tu Y.K., Yen C.Y., Ma C,.H., Yu S.W., Chou Y.C., Lee M.S., and Ueng S.W.N. (2008) Soft tissue injury management and flap reconstruction for mangled lower extremities. *Injury*, 39 (S4): 75-95.

Turner, N.J., Badylak, J.S., Weber, D.J. and Badylak, S.F. (2012). Biological scaffold in a dog model of complex musculoskeletal injury. *Journal of Surgical Research,* 1-13.

Usas, A., and Huard, J. (2007). Muscle-derived stem cells for tissue engineering and regenerative therapy. *Biomaterials,* 28: 5401-5406.

Valentin, J.E., Badylak, J.S., McCabe, G.P. and Badylak, S.F. (2006). Extracellular matrix bioscaffolds for orthopaedic applications: a comparative histologic study. *Journal of Bone and Joint Surgery*, 88 (12): 2673–2686.

Wang, Y.X., and Rudnicki, M.A., (2012). Satellite cells, the engines of muscle repair. *Nature Reviews,* 12: 127-133.

Wingate, K., Floren, M., Tan, Y., Tseng, P., and Tan, W. (2013). Synergism of matrix stiffness and vascular endothelial growth factor on mesenchymal stem cells for vascular endothelial regeneration. *Tissue Engineering Part A*. 1-10.

Wolf, M.T., Daly, K.A., Reing, J.E., and Badylak, S.F. (2012). Biological scaffold composed of skeletal muscle extracellular matrix. *Biomaterials,* 33(10): 2916-2925.

Woodbury, D., Reynolds, K., and Black, I.B. (2002). Adult bone marrow stromal stem cells express germline, ectodermal, endodermal, and mesodermal genes prior to neurogenesis. *Journal of Neuroscience Research,* 96: 908-917.

Yeghiazarians, Y., Zhang, Y., Prasad, M., Shih, H., Saini, S.A., Takagawa, J., Sievers, R.E., Wong, M.L., Kapasi, N.K., Mirsky, R., Koskenvuo, J., Minasi, P., Ye, J., Viswanathan, M. N., Angeli, F.S., Boyle, A. J., and Springer, M.L. (2009). Injection of bone marrow cell extract into infracted hearts results in functional improvement comparable to intact cell therapy. *Molecular Therapy,* 1-7.

Yu, X., Dillon, G.P., and Bellamkonda, R.V. (1999). A laminin and nerve growth factor-laden three-dimensional scaffold for enhanced neurite extension. *Tissue Engineering,* 5 (4): 291-304.

Zhang, G., and Suggs, L. J. (2007). Matrices and scaffolds for drug delivery in vascular tissue engineering. Advanced Drug Delivery Reviews, 59: 360-373.

Zhang, G., Nakamura, Y., Wang, X., Hu, Q., Suggs, L. J., & Zhang, J. (2007). Controlled Release of Stromal Cell–Derived Factor-1alphaIn SituIncreases C-kit+Cell Homing to the Infarcted Heart. *Tissue Engineering, 13*(8), 2063-2071.

Zhang, G., Hu, Q., Braunlin, E. A., Suggs, L. J., & Zhang, J. (2008). Enhancing Efficacy of Stem Cell Transplantation to the Heart with a PEGylated Fibrin Biomatrix. *Tissue Engineering Part A, 14*(6), 1025-1036.

Zouris JM, Walker GJ, Dye J. Galarneau M. 2006. Wounding patterns for U.S. Marines and sailors during Operation Iraqi Freedom, major combat phase. *Military Medicine.* 171 (3): 246-52.

Zuker, R.M. and Maktelow, R.T. (2007). Functioning free muscle transfers. *Hand Clinics,* 23 (1): 57-72.